

SUPPORTING INFORMATION

The Influence of Nitrogen Doping of the Acceptor in Orange–Red Thermally Activated Delayed Fluorescence Emitters and OLEDs

*Changfeng Si,^{a†} Ya-Nan Hu,^{b†} Dianming Sun,^a Kai Wang^b, Xiao-Hong Zhang^{*bc} and Eli Zysman-Colman^{*a}*

^a Organic Semiconductor Centre, EaStCHEM School of Chemistry, University of St Andrews, St Andrews KY16 9ST, UK. eli.zysman-colman@st-andrews.ac.uk.

^b Institute of Functional Nano & Soft Materials (FUNSOM), Joint International Research Laboratory of Carbon-Based Functional Materials and Devices, Soochow University, Suzhou, Jiangsu 215123, P. R. China. xiaohong_zhang@suda.edu.cn

^c Jiangsu Key Laboratory of Advanced Negative Carbon Technologies, Soochow University, Suzhou, 215123, Jiangsu, PR China

[†] *Equal Contribution*

Key words: nitrogen doping, polycyclic aromatic hydrocarbons, thermally activated delayed fluorescence, dibenzo[a,c]phenazine, red emitter, organic light-emitting diode

Contents

1. General Methods	S3
2. Experimental Section.....	S8
3. DFT Calculations	S31
4. Photophysical Properties.....	S35
5. OLED Fabrication and Characterization.....	S45
6. References	S48

1. General Methods

General Synthetic Procedures

All commercially available chemicals and reagent grade solvents were used as received. 5-(9,9-dimethylacridin-10(9H)-yl)benzo[*c*][1,2,5]thiadiazole (**DMACPhSN**) was synthesised according to the literature.¹ Air-sensitive reactions were performed under a nitrogen atmosphere using Schlenk techniques. Flash column chromatography was carried out using silica gel (Silia-P from Silicycle, 60 Å, 40-63 µm). Analytical thin-layer-chromatography (TLC) was performed with silica plates with aluminum backings (250 µm with F-254 indicator). TLC visualization was accomplished by 254/365 nm UV lamp. HPLC analysis was conducted on a Shimadzu Prominence Modular HPLC system. HPLC traces were performed using an ACE Excel 2 C18 analytical column. ¹H and ¹³C NMR spectra were recorded on a Bruker Advance spectrometer (400 or 500 MHz for ¹H, 101 or 126 MHz for ¹³C). The following abbreviations have been used for multiplicity assignments: “s” for singlet, “d” for doublet, “t” for triplet, “dd” for doublet of doublets, “dt” for doublet of triplets, “ddd” for doublet of doublet of doublets, “q” for quintet and “m” for multiplet. Deuterated chloroform (CDCl₃) or DMSO-*d*₆ was used as the solvent of record. ¹H NMR and ¹³C NMR spectra were referenced to the solvent peak. Melting points were measured using open-ended capillaries on an Electrothermal 1101D Mel-Temp apparatus and are uncorrected. High-resolution mass spectrometry (HRMS) was performed at the University of Edinburgh. Elemental analyses were performed by the School of Geosciences at the University of Edinburgh.

Theoretical Calculations

Density functional theoretical (DFT) calculation and time-dependent density functional theoretical (TDDFT) calculations were performed using Gaussian 16 Revision D.01 software in the gas phase.² The ground-state geometries were optimized employing the PBE0³ functional with the Pople 6-31G(d,p) basis set, in the gas phase.⁴ Transitions to excited singlet states and triplet states were calculated using TDDFT within the Tamm-Dancoff approximation (TDA) based on the optimized ground-state geometries.^{5,6} Molecular orbitals were visualized using GaussView 6.0⁷ and Silico 2.1, an in-house built software package.⁸⁻¹⁵ Hole-electron and reduced density gradient (RDG)¹⁶ analyses were conducted using the Multiwfn program,¹⁷ and

the corresponding molecular orbitals were visualized using VMD program.⁸

Electrochemistry measurements.

Cyclic Voltammetry (CV) and differential pulse voltammetry (DPV) analysis were performed on an Electrochemical Analyzer potentiostat model 620E from CH Instruments. Samples were prepared in dichloromethane (DCM) solutions, which were degassed by sparging with DCM-saturated nitrogen gas for 5 minutes prior to measurements. All measurements were performed using 0.1 M tetra-*n*-butylammonium hexafluorophosphate, [*n*Bu₄N]PF₆, in DCM. An Ag/Ag⁺ electrode was used as the reference electrode, a platinum electrode was used as the working electrode and a platinum wire was used as the counter electrode. The redox potentials are reported relative to a saturated calomel electrode (SCE) with a ferrocene/ferrocenium (Fc/Fc⁺) redox couple as the internal standard (0.46 V vs SCE).¹⁸ The HOMO and LUMO energies were calculated using the relation $E_{\text{HOMO/LUMO}} = -(E_{\text{ox}}/E_{\text{red}} \text{ vs Fc/Fc}^+ + 4.8) \text{ eV}$,¹⁹ where E_{ox} and E_{red} are anodic and cathodic peak potentials obtained from DPV, respectively, versus Fc/Fc⁺.

Photophysical Measurements

All samples were prepared in HPLC grade toluene (PhMe), Diethyl ether (Et₂O), dichloromethane (DCM) or acetonitrile (MeCN) with varying concentrations on the order of 10⁻⁵ or 10⁻⁶ M for absorption and emission study. Absorption spectra were recorded at RT using a Shimadzu UV-2600 double beam spectrophotometer. Molar absorptivity determination was verified by linear least-squares fit of values obtained from at least five independent solutions at varying concentrations with absorbance ranging from 1.0×10^3 to $1.3 \times 10^4 \text{ M}^{-1} \text{ cm}^{-1}$ for **DMACBP**, 0.4×10^3 to $2.3 \times 10^4 \text{ M}^{-1} \text{ cm}^{-1}$ for **DMACPyBP**, 0.5×10^3 to $2.4 \times 10^4 \text{ M}^{-1} \text{ cm}^{-1}$ for **DMACBPN**, 0.6×10^3 to $1.7 \times 10^4 \text{ M}^{-1} \text{ cm}^{-1}$ for **DMACPyBPN**.

Degassed solutions were prepared via three freeze-pump-thaw cycles prior to emission analysis using an in-house adapted fluorescence cuvette, itself purchased from Starna. Steady-state emission and time-resolved emission spectra were recorded at 298 K using an Edinburgh Instruments FS5 fluorimeter. All the samples for the steady-state measurements were excited at 375 nm using a Xenon lamp. Phosphorescence emission spectra were collected with a 5 W microsecond flash lamp using the multi-channel scaling (MCS) mode with a gate time of 1-10 ms. The short-time ranges (1-200 ns, 1 ns-50 μ s) of the PL decays were measured using time-correlated single photon counting (TCSPC) mode by 5 mW EPL-375 picosecond pulsed laser. The long-time ranges (1 ns-200 μ s, 1 ns-2 ms) of the PL decays were measured using multi-

channel scaling (MCS) mode.

Photoluminescence quantum yields for solutions were excited at 390 nm for all compounds and determined using the optically dilute method.^{20,21} The Beer-Lambert law was found to be linear at the concentrations of the solutions. For each sample, linearity between absorption and emission intensity was verified through linear regression analysis and additional measurements were acquired until the Pearson regression factor (R^2) for the linear fit of the data set surpassed 0.9. Individual relative quantum yield values were calculated for each solution and the values reported represent the gradient value. The equation $\Phi_s = \Phi_r(A_r/A_s)(I_s/I_r)(n_s/n_r)^2$ was used to calculate the relative quantum yield of each of the sample, where Φ_r is the absolute quantum yield of the reference, n is the refractive index of the solvent, A is the absorbance at the excitation wavelength, and I is the integrated area under the corrected emission curve. The subscripts s and r refer to the sample and reference, respectively. A solution of quinine sulfate ($\Phi_r = 54.6\%$ in 1 N H_2SO_4)²² was used as the external reference. An integrating sphere (SC-30 module on FS5 fluorimeter) was employed for the photoluminescence quantum yield measurements of solid samples. The Φ_{PL} of the films were then measured in air and N_2 environment by purging the integrating sphere with N_2 gas flow.

The singlet-triplet splitting energy, ΔE_{ST} , was estimated by recording the prompt fluorescence and the delayed emission spectra at 77 K. The 77 K glass samples were prepared by transferring toluene solution into NMR tubes and the NMR tubes were cooled down inside a suprasil nitrogen dewar flask by liquid nitrogen. Prompt fluorescence spectra were measured using time resolved emission spectroscopy (TRES) with a 5 mW EPL-375 picosecond pulsed laser. Phosphorescence spectra of 2-MeTHF glass at 77 K were acquired by exciting the sample with a 5 W microsecond flash lamp and measuring the time-gated (1-10 ms) emission.

Fitting of the time-resolved luminescence measurements:

Time-resolved PL measurements were fitted to a sum of exponentials decay model, with chi-squared (χ^2) values of between 1 and 2, using the EI FS5 software. Each component of the decay is assigned a weight, (w_i), which is the contribution of the emission from each component to the total emission.

The average lifetime was then calculated using the following:

- Two exponential decay model:

$$\tau_{AVG} = \tau_1 w_1 + \tau_2 w_2$$

with weights defined as $w_1 = \frac{A_1 \tau_1}{A_1 \tau_1 + A_2 \tau_2}$ and $w_2 = \frac{A_2 \tau_2}{A_1 \tau_1 + A_2 \tau_2}$ where A_1 and A_2 are the preexponential-factors of each component.

- Three exponential decay model:

$$\tau_{AVG} = \tau_1 w_1 + \tau_2 w_2 + \tau_3 w_3$$

with weights defined as $w_1 = \frac{A_1 \tau_1}{A_1 \tau_1 + A_2 \tau_2 + A_3 \tau_3}$, $w_2 = \frac{A_2 \tau_2}{A_1 \tau_1 + A_2 \tau_2 + A_3 \tau_3}$ and $w_3 = \frac{A_3 \tau_3}{A_1 \tau_1 + A_2 \tau_2 + A_3 \tau_3}$ where A_1 , A_2 and A_3 are the preexponential-factors of each component.

OLED fabrication and characterization

OLED devices were fabricated in bottom-emitting architecture. A pre-patterned indium tin oxide (ITO) glass substrate with a sheet resistance of $15 \Omega \text{ square}^{-1}$ was pre-cleaned carefully with detergent and deionized water and then exposed to UV-ozone for 15 min. The small molecules for each layer were thermally evaporated using a vacuum chamber with a base pressure of $4 \times 10^{-4} \text{ Pa}$ and deposited at a rate of 1 \AA/s , which was controlled in situ using the quartz crystal monitors. The electron injection layer, LiF, was deposited at a rate of 0.1 \AA/s while the Al cathode was deposited at a rate of 10 \AA/s through the shadow mask defining the top electrode. The spatial overlap of the anode and cathode electrodes determined the active area of the OLED, which was estimated to be 9 mm^2 . Electroluminescence (EL), CIE colour coordinates, and spectra were obtained via a Spectrascan PR655 photometer and the luminance-current-voltage characteristics were determined with a computer-controlled Keithley 2400 Source meter. The external quantum yield (EQE) was calculated from the current density, luminance, and EL spectrum, assuming a Lambertian emission distribution.

Literature study

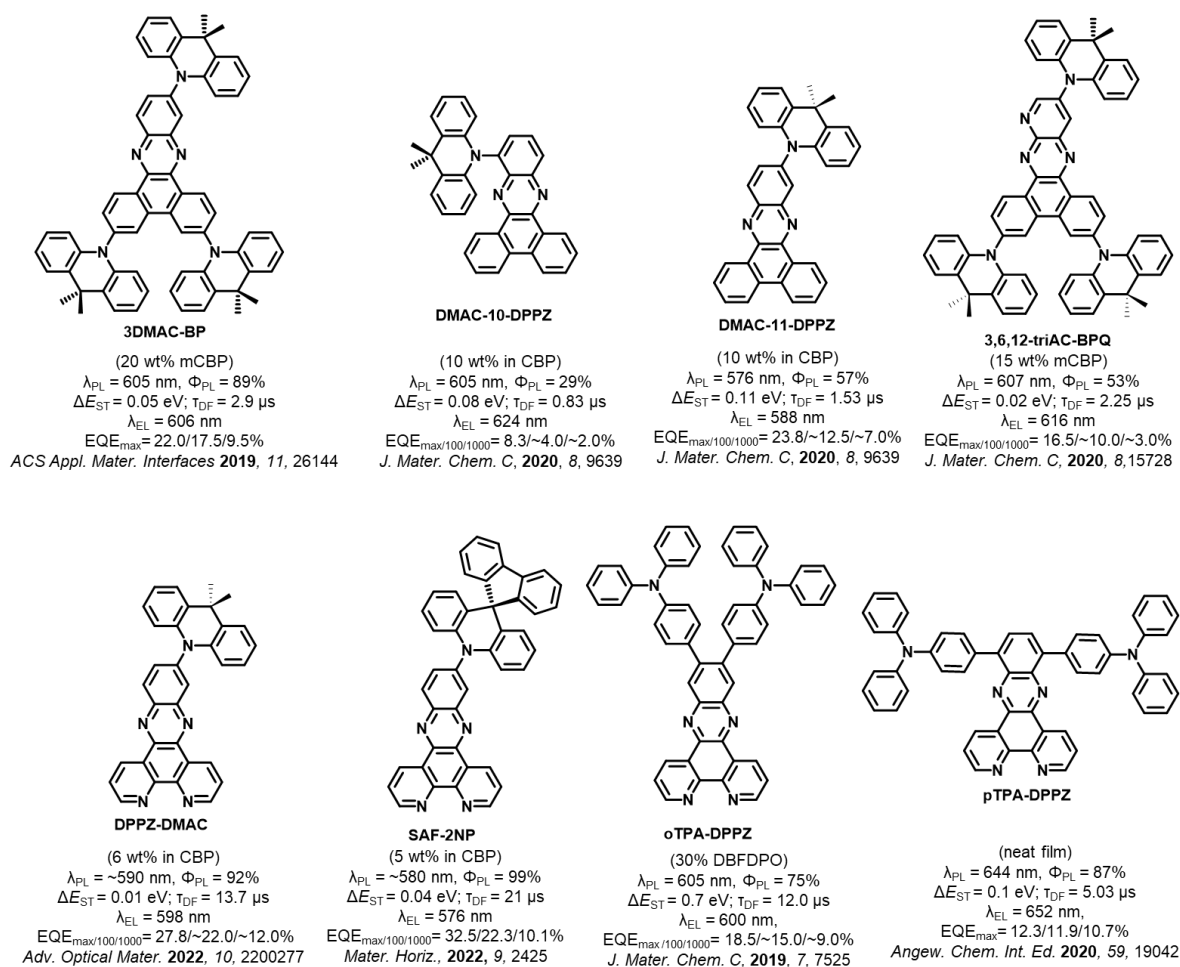
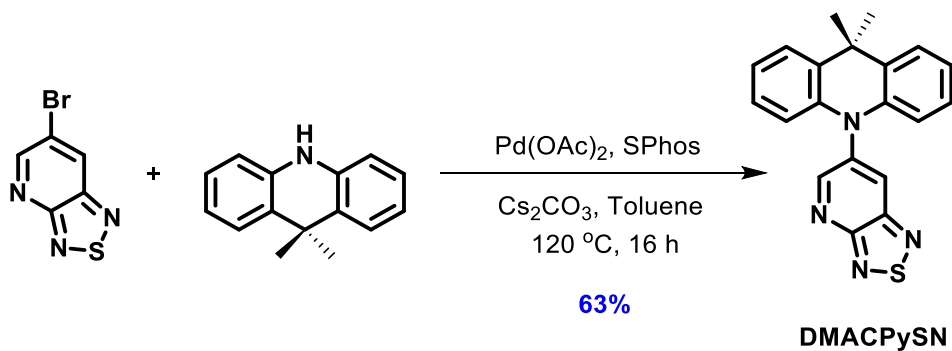


Figure S1. Molecular structures of the emitters discussed in the introduction.

2. Experimental Section

Synthesis of 6-(9,9-dimethylacridin-10(9*H*)-yl)-[1,2,5]thiadiazolo[3,4-*b*]pyridine (DMACPySN):



6-Bromo-[1,2,5]thiadiazolo[3,4-*b*]pyridine (2.00 g, 9.26 mmol, 1.0 equiv.), DMAC (2.13 g, 10.18 mmol, 1.1 equiv.), cesium carbonate (9.05 g, 27.77 mmol, 3.0 equiv.), 2-dicyclohexylphosphino-2',6'-dimethoxybiphenyl (0.23 g, 0.56 mmol, 0.06 equiv.), and palladium(II) acetate (62 mg, 0.28 mmol, 0.03 equiv.) were dissolved in 40 mL of dry toluene and the flask placed under N₂. The mixture was stirred at 120 °C for 16 h. The resulting mixture was cooled to room temperature and then poured into water (30 mL). The organic phase was extracted with DCM (3 × 100 mL). The combined organic layers were dried over anhydrous magnesium sulfate and concentrated under reduced pressure. The crude product was purified by column chromatography on silica gel (17% DCM/Hexane) to afford **DMACPySN** as a red solid (yield = 2.00 g).

6-(9,9-dimethylacridin-10(9*H*)-yl)-[1,2,5]thiadiazolo[3,4-*b*]pyridine (DMACPySN): R_f = 0.3 (17% DCM/Hexane). **Yield:** 63%. **Mp** = 175-176 °C. ¹H NMR (400 MHz, CDCl₃) δ 9.02 (d, *J* = 2.5 Hz, 1H), 8.47 (d, *J* = 2.5 Hz, 1H), 7.61 – 7.49 (m, 2H), 7.09 – 7.02 (m, 4H), 6.42 – 6.31 (m, 2H), 1.75 (s, 6H). ¹³C NMR (101 MHz, CDCl₃) δ 160.76, 159.30, 148.25, 140.08, 138.10, 131.44, 131.05, 126.74, 125.74, 122.17, 114.39, 77.36, 77.05, 76.73, 36.22, 30.91. GC-MS Calculated: (C₂₁H₁₇N₃S) 344.11; Found: 344.16, Retention time: 12.42 minutes in DCM.

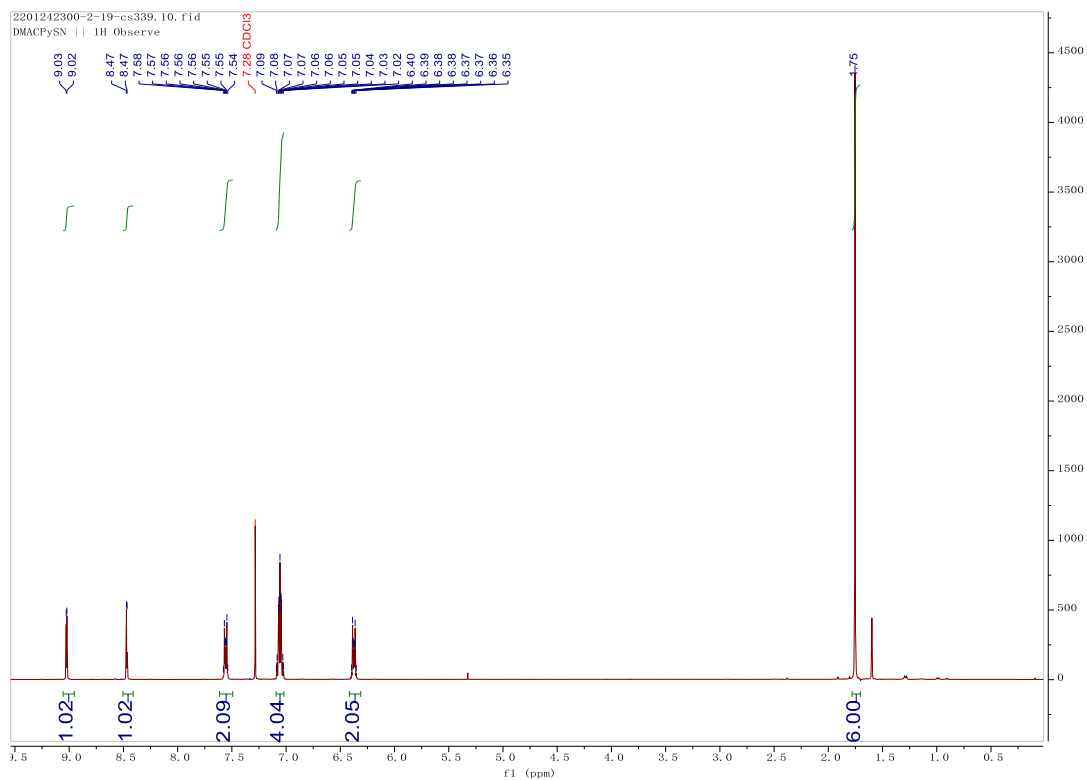


Figure S2. ^1H NMR spectra of **DMACPySN** in CDCl_3 .

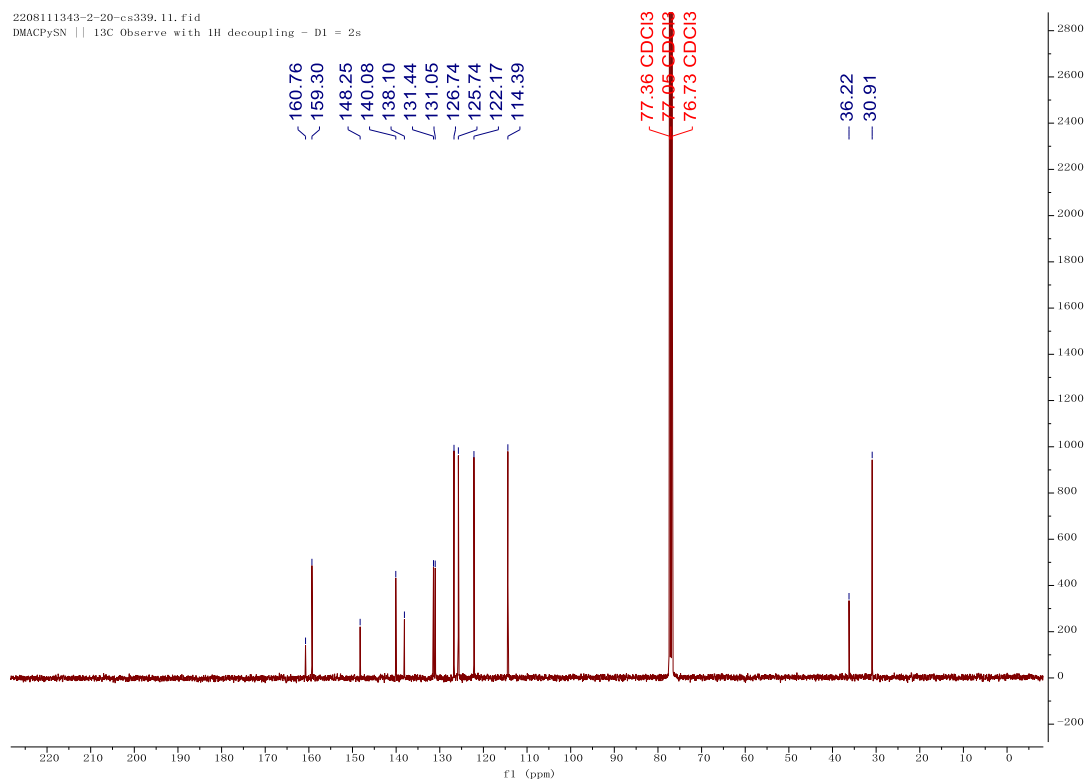


Figure S3. ^{13}C NMR spectra of **DMACPySN** in CDCl_3 .

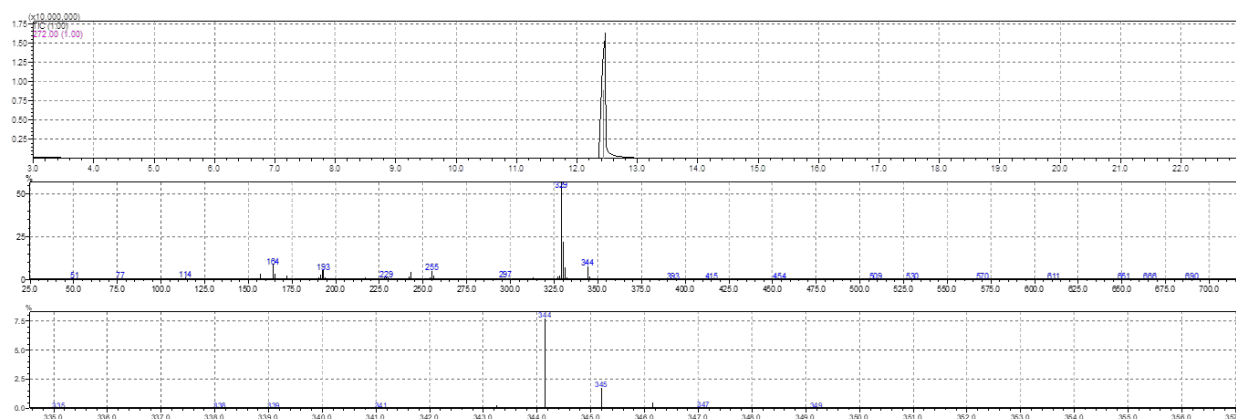
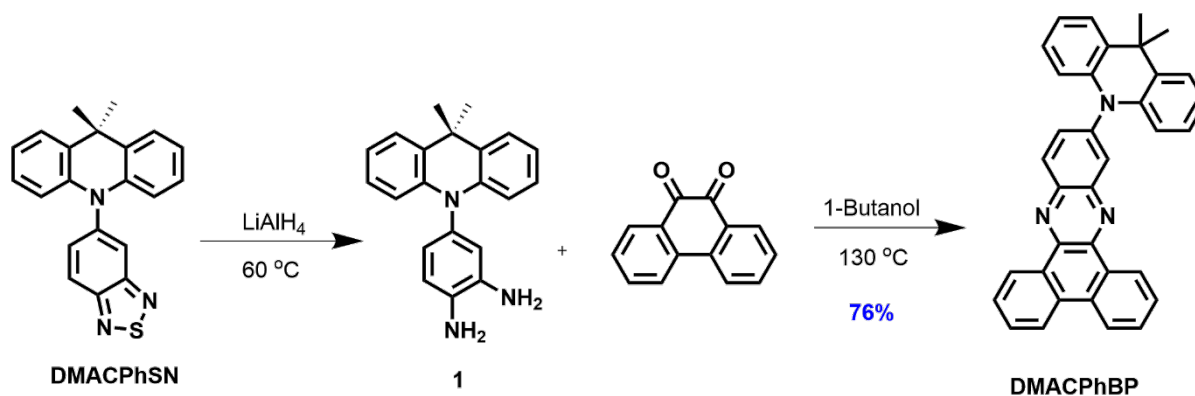


Figure S4. GCMS of DMACPySN.

Synthesis of 11-(9,9-dimethylacridin-10(9*H*)-yl)dibenzo[*a,c*]phenazine (DMACBP):



To a solution of **DMACPhSN** (0.5 g, 1.46 mmol, 1.0 equiv.) in dry THF (20 mL) was added lithium aluminum hydride (0.44 g, 11.65 mmol 8.0 equiv.) under a continuous N₂ flow. The resulting mixture was stirred at 60 °C under a N₂ atmosphere for 2 h. After cooling to 0 °C, the reaction mixture was quenched with water (2 mL) and then 2 M NaOH(aq) (2 mL). The above solution was filtered through a pad of Celite, which was subsequently rinsed with ethyl acetate, and the filtrate was then extracted with ethyl acetate (3×30 mL). The organic layer was collected and dried over MgSO₄. After filtration and removal of the solvent, compound **1** was used directly for the next step without further purification. Compound **1** and phenanthrene-9,10-dione (0.30 g, 1.46 mmol, 1.0 equiv.) were added into 20 mL of 1-butanol and then heated to reflux for 12 hours under a N₂ atmosphere. After cooling to room temperature, the solution was poured into water and extracted with DCM (3 × 100 mL). The organic layer was dried over Na₂SO₄ and concentrated under reduced pressure. The residue was purified by column chromatography with (25% DCM/Hexane) to afford the compound **DMACBP** as yellow solid

(0.54 g).

11-(9,9-dimethylacridin-10(9H)-yl)dibenzo[*a,c*]phenazine (DMACBP): $R_f = 0.3$ (25% DCM/Hexane). **Yield:** 76%. **Mp** = 257-258 °C. $^1\text{H NMR}$ (500 MHz, CDCl_3) δ 9.49 (dd, $J = 8.0, 1.5$ Hz, 1H), 9.41 (dd, $J = 8.1, 1.4$ Hz, 1H), 8.73 – 8.57 (m, 3H), 8.45 (d, $J = 2.2$ Hz, 1H), 7.91 – 7.75 (m, 5H), 7.58 – 7.51 (m, 2H), 7.04 – 6.96 (m, 4H), 6.52 – 6.39 (m, 2H), 1.79 (s, 6H). $^{13}\text{C NMR}$ (126 MHz, CDCl_3) δ 143.25, 142.76, 142.40, 141.66, 140.69, 132.98, 132.30, 131.41, 130.72, 130.68, 130.64, 128.12, 126.49, 126.44, 125.31, 123.04, 121.15, 114.60, 77.28, 77.02, 76.77, 36.17, 31.06. **HR-MS** $[\text{M}+\text{H}]^+$ **Calculated:** ($\text{C}_{35}\text{H}_{25}\text{N}_3$) 487.2048; **Found:** 487.2043. **Anal. Calcd. for $\text{C}_{35}\text{H}_{25}\text{N}_3$:** C, 86.21%; H, 5.17%; N, 8.62%. **Found:** C, 85.78%; H, 5.11%; N, 8.47%. **HPLC analysis:** 99.04% pure on HPLC analysis, retention time 10.0 minutes in 90% Acetonitrile 10% water.

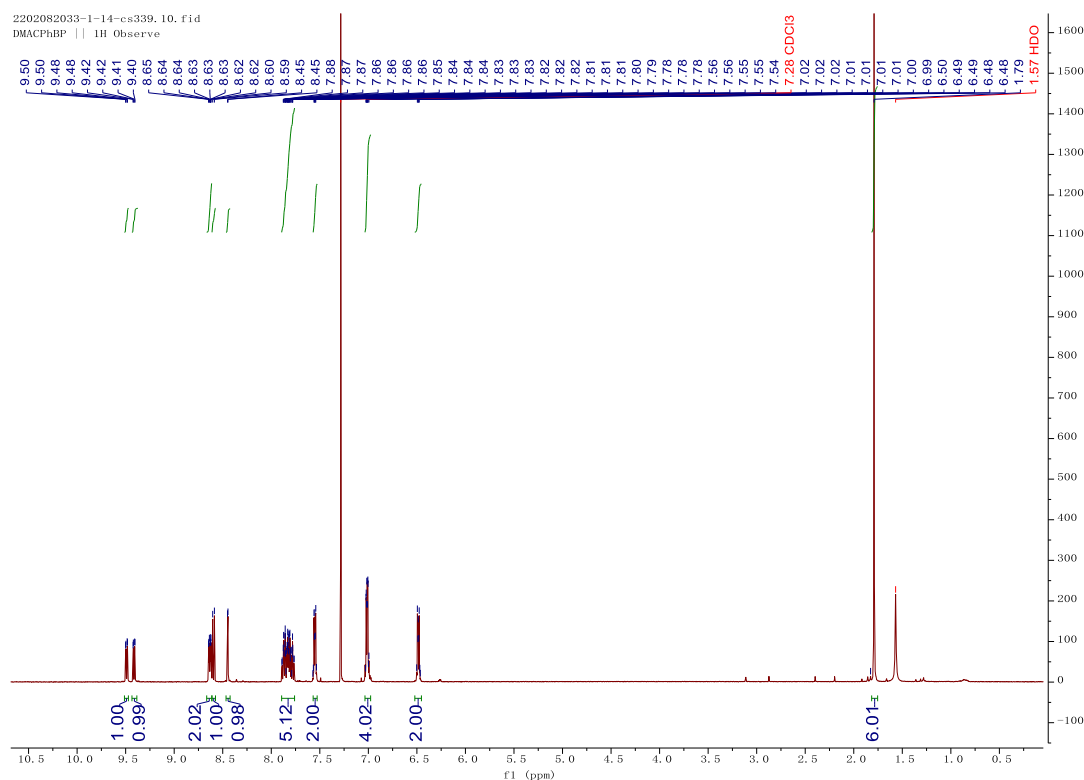


Figure S5. $^1\text{H NMR}$ spectra of **DMACBP** in CDCl_3 .

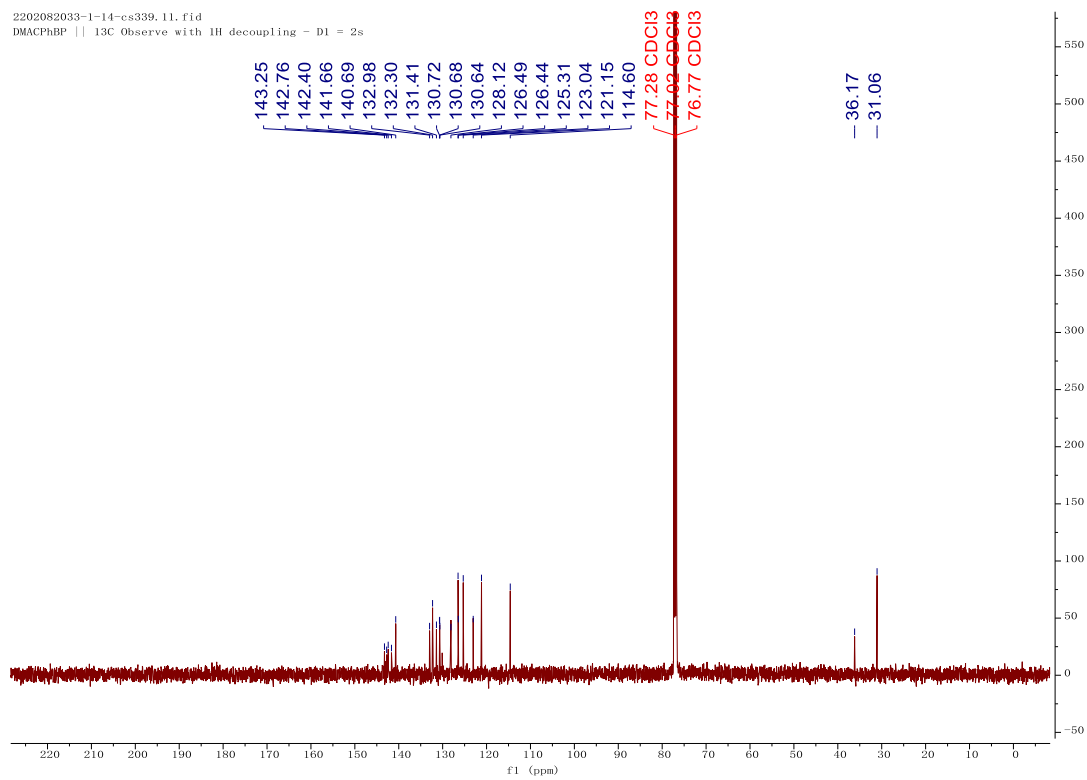
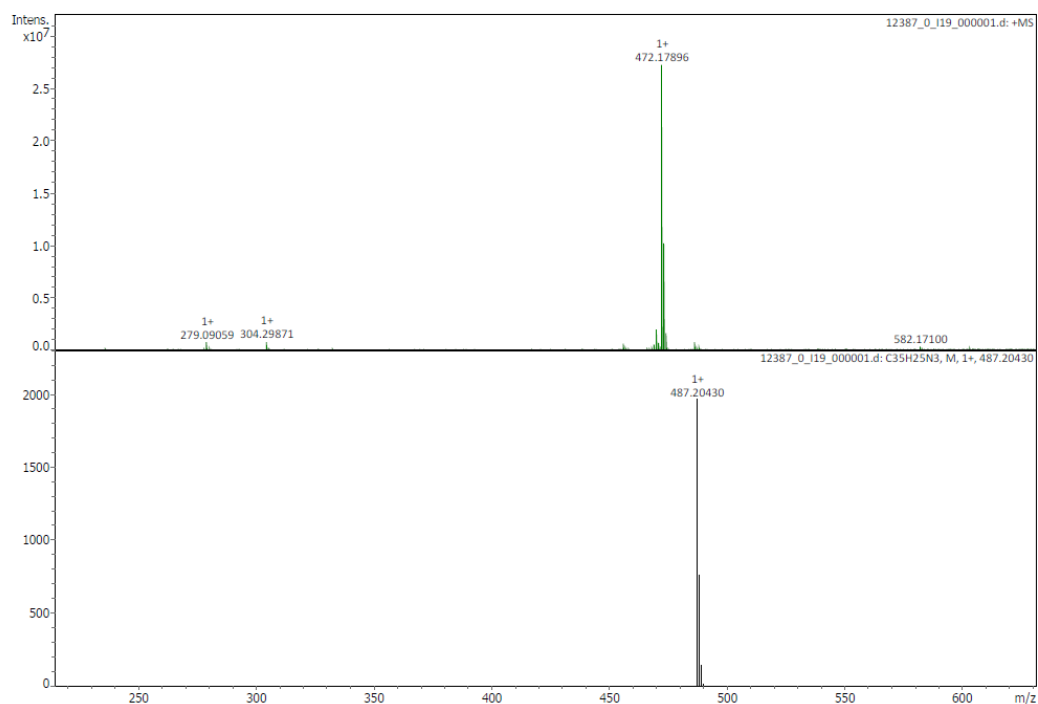


Figure S6. ^{13}C NMR spectra of **DMACBP** in CDCl_3 .

Generic Display Report (all)



Bruker Compass DataAnalysis 5.3

printed: 15-Mar-22 3:22:06 PM

by: demo

Page 1 of 1

Figure S7. HRMS of DMACBP.

Elemental Analysis Service Request Form

Researcher name Changfeng Si

Researcher email cs339@st-andrews.ac.uk

NOTE: Please submit ca. 10 mg of sample

Sample reference number	CFS-230-DMACBP
Name of Compound	DMACBP
Molecular formula	C35H25N3
Stability	
Hazards	
Other Remarks	

Analysis type:

Single Duplicate Triplicate

Analysis Result:

Element	Expected %	Found (1)	Found (2)	Found (3)
Carbon	86.21	84.78	85.78	
Hydrogen	5.17	5.11	5.23	
Nitrogen	8.62	8.38	8.47	
Oxygen				

Authorising Signature:

Date completed	30-03-22
Signature	J-PL
comments	-

Figure S8. EA of DMACBP.

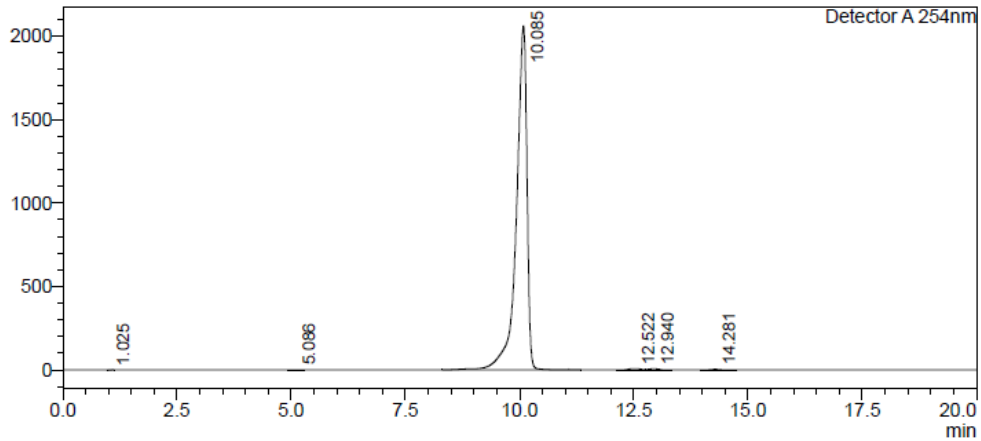
HPLC Trace Report24Feb2022

<Sample Information>

Sample Name : DMACBPB
 Sample ID :
 Method Filename : 90% Acetonitrile 10 Water 20 mins.lcm
 Batch Filename : DMACBP.lcb
 Vial # : 1-11 Sample Type : Unknown
 Injection Volume : 5 uL
 Date Acquired : 24/02/2022 13:55:24 Acquired by : System Administrator
 Date Processed : 24/02/2022 14:15:26 Processed by : System Administrator

<Chromatogram>

mV

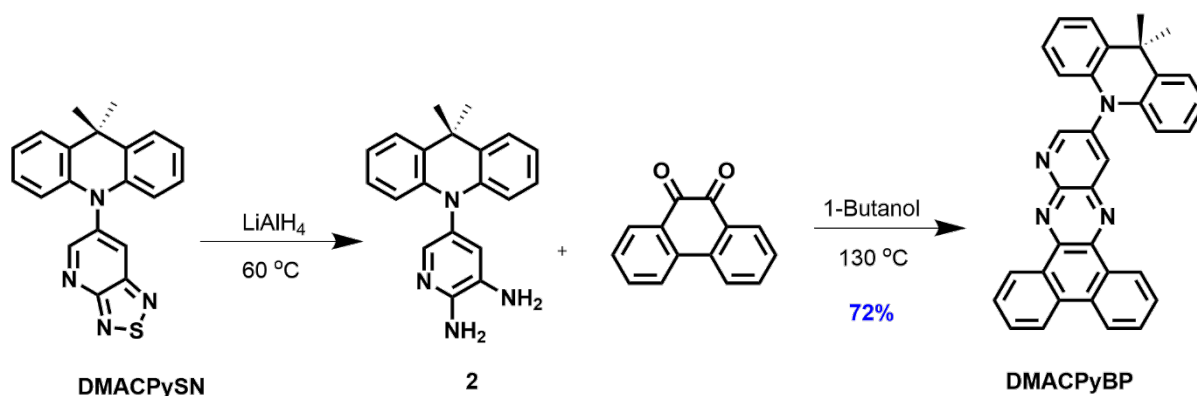


<Peak Table>

Detector A 254nm							
Peak#	Ret. Time	Area	Height	Area%	Area/Height	Width at 5% Height	
1	1.025	4405	1168	0.013	3.770	--	
2	5.086	16955	2157	0.050	7.861	0.259	
3	10.085	33284932	2060182	99.044	16.156	0.654	
4	12.522	127079	6758	0.378	18.804	--	
5	12.940	101215	5912	0.301	17.119	--	
6	14.281	71741	3835	0.213	18.705	0.604	
Total		33606326	2080013	100.000			

Figure S9. HPLC trace of DMACBP.

Synthesis of 12-(9,9-dimethylacridin-10(9H)-yl)dibenzo[*f,h*]pyrido[2,3-*b*]quinoxaline (DMACPyBP):



Compound **DMACPyBP** was synthesized according to the same procedure as described above for the synthesis of **DMACBP**, except that **DMACPySN** (2.2 g, 5.3 mmol) was used as the reactant instead of **DMACPhSN**, yielding a red solid (Yield = 0.515 g).

12-(9,9-dimethylacridin-10(9H)-yl)dibenzo[*f,h*]pyrido[2,3-*b*]quinoxaline (DMACPyBP):
 R_f = 0.3 (33% DCM/Hexane). **Yield:** 72%. **Mp** = 241-243 $^\circ\text{C}$. **^1H NMR (500 MHz, DMSO- d_6)** δ 9.36 (dd, J = 8.0, 1.5 Hz, 1H), 9.29 – 9.24 (m, 2H), 8.99 (d, J = 2.6 Hz, 1H), 8.92 – 8.84 (m, 2H), 8.02 – 7.83 (m, 4H), 7.63 – 7.58 (m, 2H), 7.07 – 7.00 (m, 4H), 6.49 – 6.44 (m, 2H), 1.72 (s, 6H) ppm. **^{13}C NMR (126 MHz, DMSO- d_6)** δ 158.25, 144.54, 143.28, 140.43, 139.90, 138.43, 138.39, 132.66, 132.42, 132.18, 132.01, 131.20, 129.68, 129.32, 129.16, 129.06, 127.25, 126.71, 126.44, 126.25, 124.38, 122.09, 115.02, 36.29, 31.68 ppm. **HR-MS (Xevo G2-S) [M+H] $^+$ Calculated:** ($\text{C}_{34}\text{H}_{24}\text{N}_4$) 488.2001; **Found:** 488.2054. **Anal. Calcd. for $\text{C}_{34}\text{H}_{24}\text{N}_4$:** C, 83.58%; H, 4.95%; N, 11.47%. **Found:** C, 83.57%; H, 4.99%; N, 11.19%. **HPLC analysis:** 98.8% pure on HPLC analysis, retention time 9.11 minutes in 80% MeOH 20% water.

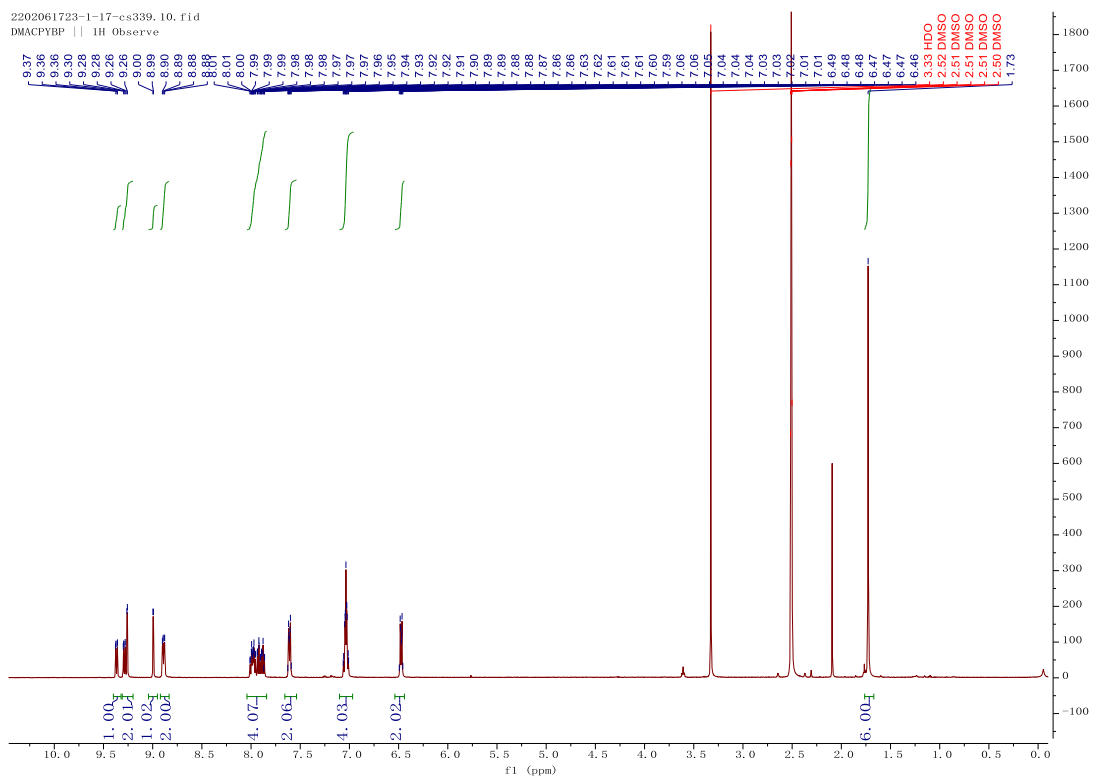


Figure S10. ^1H NMR spectra of DMACPyBP in $\text{DMSO-}d_6$.

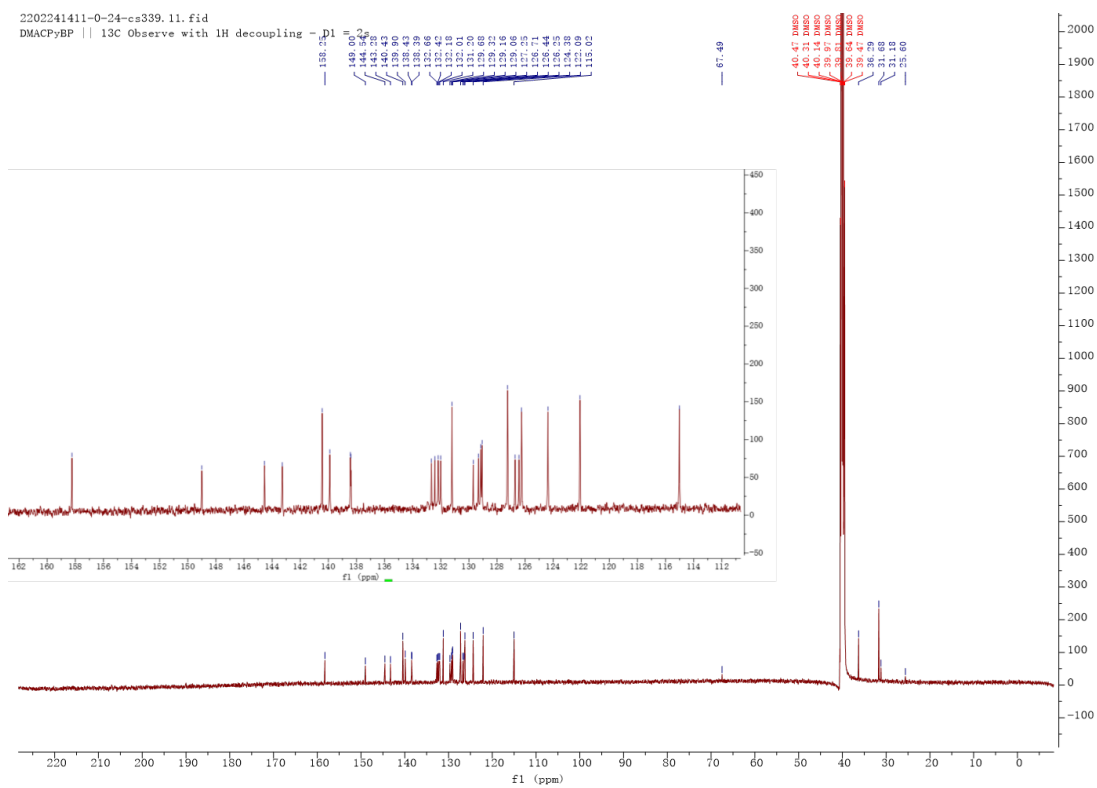


Figure S11. ^{13}C NMR spectra of DMACPyBP in $\text{DMSO-}d_6$.

Generic Display Report (all)

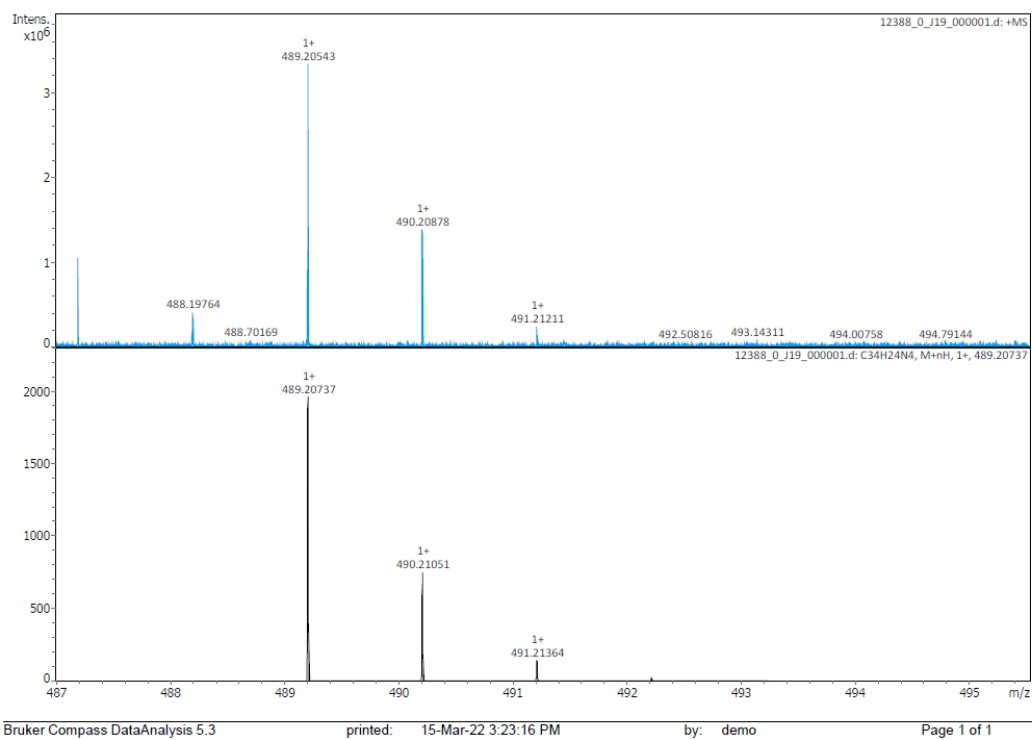


Figure S12. HRMS of DMACPyBP.

Elemental Analysis Service Request Form

Researcher name Changfeng Si

Researcher email cs339@st-andrews.ac.uk

NOTE: Please submit ca. 10 mg of sample

Sample reference number	CFS-231-DMACPyBP
Name of Compound	DMACPyBP
Molecular formula	C34H24N4
Stability	
Hazards	
Other Remarks	

Analysis type:

Single Duplicate Triplicate

Analysis Result:

Element	Expected %	Found (1)	Found (2)	Found (3)
Carbon	83.58	83.57	83.61	
Hydrogen	4.95	5.42	4.99	
Nitrogen	11.47	11.18	11.19	
Oxygen				

Authorising Signature:

Date completed	30.03.22
Signature	S-P-C
comments	-

Figure S13. EA of DMACPyBP.

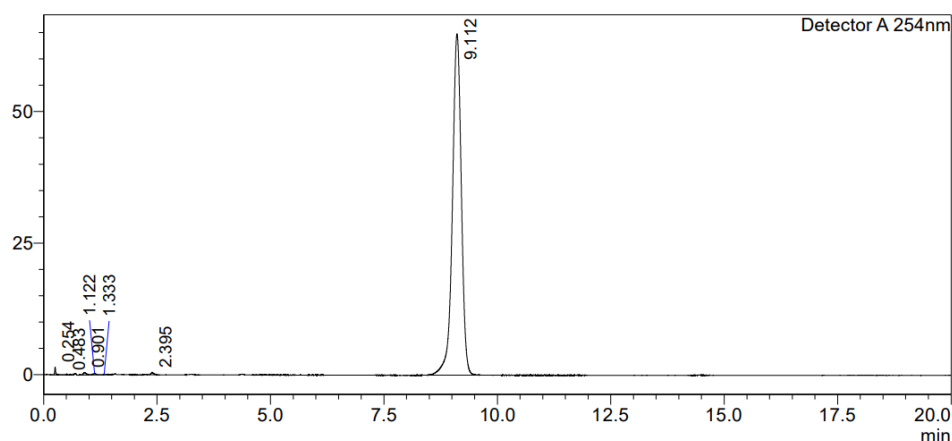
HPLC Trace Report 14 Oct 2021

<Sample Information>

Sample Name : DMACPyBP
Sample ID :
Method Filename : 80% Methanol 20 Water 20 mins.lcb
Batch Filename : DMACPyBP.lcb
Vial # : 1-2
Injection Volume : 5 uL
Date Acquired : 14/10/2021 15:02:41
Date Processed : 14/10/2021 15:22:44
Sample Type : Unknown
Acquired by : System Administrator
Processed by : System Administrator

<Chromatogram>

mV



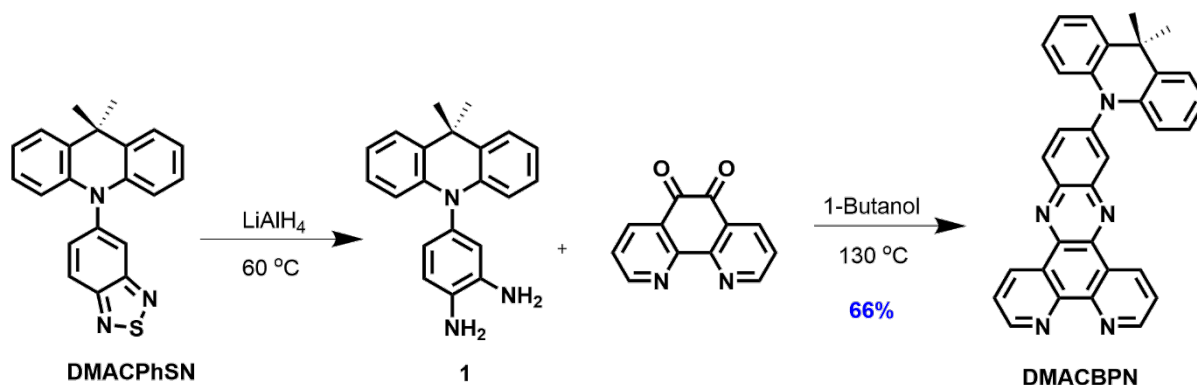
<Peak Table>

Detector A 254nm

Peak#	Ret. Time	Area	Height	Area%	Area/Height	Width at 5% Height
1	0.254	2393	1389	0.266	1.722	0.066
2	0.483	1304	75	0.145	17.451	--
3	0.901	2685	477	0.298	5.628	--
4	1.122	1392	244	0.155	5.704	--
5	1.333	1076	76	0.120	14.100	--
6	2.395	1801	387	0.200	4.655	0.160
7	9.112	889385	64815	98.817	13.722	0.485
Total		900035	67463	100.000		

Figure S14. HPLC trace of DMACPyBP.

Synthesis of 11-(9,9-dimethylacridin-10(9*H*)-yl)dipyrido[3,2-*a*:2',3'-*c*]phenazine (DMACBPN):



Compound **DMACBPN** was synthesized according to the same procedure as described above for the synthesis of **DMACBP**, except that 1,10-phenanthroline-5,6-dione (0.306 g, 1.46 mmol) was used as the reactant instead of phenanthrene-9,10-dione, yielding a red solid (Yield = 0.470 g).

11-(9,9-dimethylacridin-10(9*H*)-yl)dipyrido[3,2-*a*:2',3'-*c*]phenazine (DMACBPN): $R_f = 0.3$ (20% DCM/Hexane). **Yield:** 86%. **Mp** = $312\text{--}313\text{ }^\circ\text{C}$. **$^1\text{H NMR}$ (400 MHz, CDCl_3)** δ 9.74 (dd, $J = 8.1, 1.8\text{ Hz}$, 1H), 9.66 (dd, $J = 8.1, 1.8\text{ Hz}$, 1H), 9.34 (ddd, $J = 6.5, 4.5, 1.8\text{ Hz}$, 2H), 8.62 (dd, $J = 8.9, 0.5\text{ Hz}$, 1H), 8.48 (dd, $J = 2.3, 0.5\text{ Hz}$, 1H), 7.98 – 7.76 (m, 3H), 7.56 (dd, $J = 6.0, 3.3\text{ Hz}$, 2H), 7.09 – 6.98 (m, 4H), 6.55 – 6.47 (m, 2H), 1.78 (s, 6H). **$^{13}\text{C NMR}$ (101 MHz, CDCl_3)** δ 152.82, 152.75, 143.69, 143.54, 141.90, 140.55, 134.03, 133.68, 132.38, 131.32, 130.68, 127.58, 127.49, 126.52, 125.42, 124.39, 121.54, 114.91, 77.35, 77.04, 76.72, 36.27, 30.93. **HR-MS** (Xevo G2-S) $[\text{M}+\text{H}]^+$ **Calculated:** ($\text{C}_{33}\text{H}_{23}\text{N}_5$) 489.1953; **Found:** 489.2026. **Anal. Calcd. for $\text{C}_{33}\text{H}_{23}\text{N}_5$:** C, 80.96%; H, 4.74%; N, 14.31%. **Found:** C, 81.09%; H, 4.73%; N, 13.81%. **HPLC analysis:** 99.57% pure on HPLC analysis, retention time 3.8 minutes in 98% Methanol 2% water.

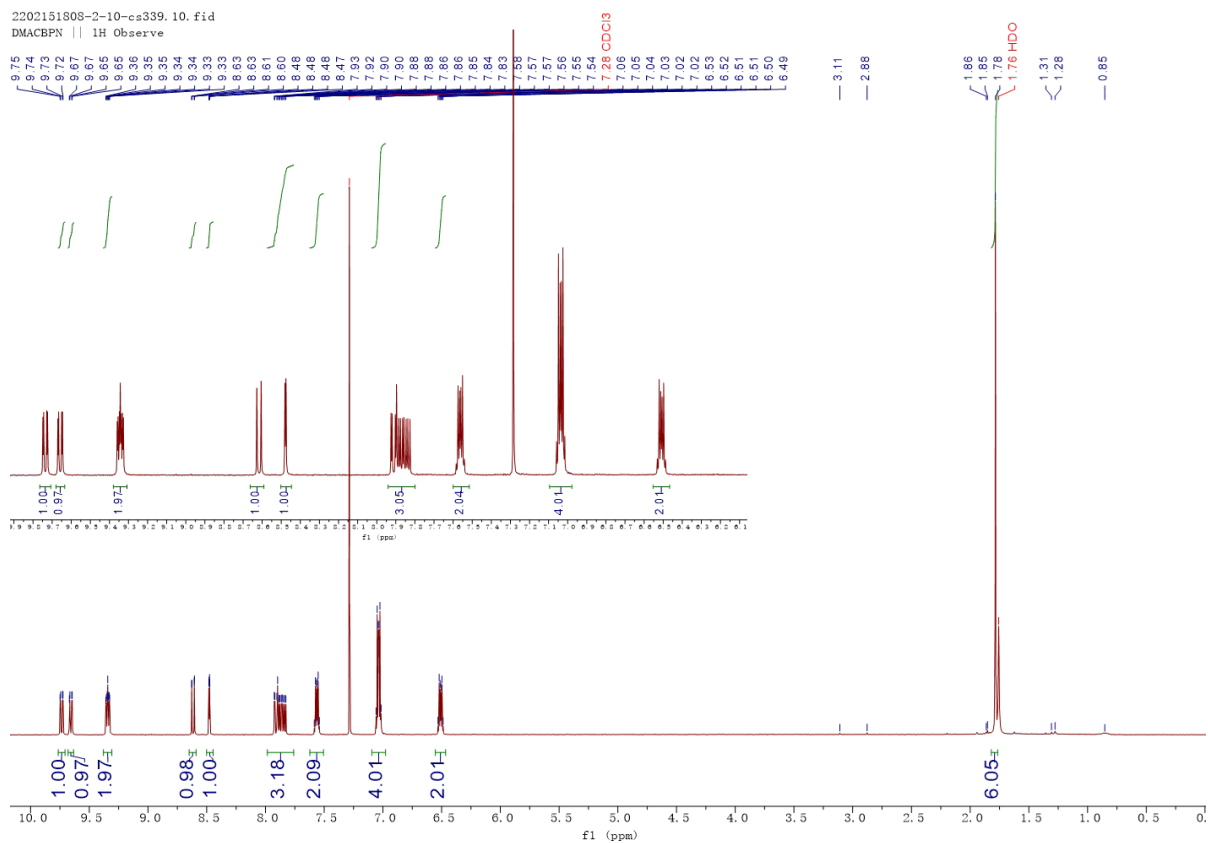


Figure S15. ^1H NMR spectra of DMACBPN in CDCl_3 .

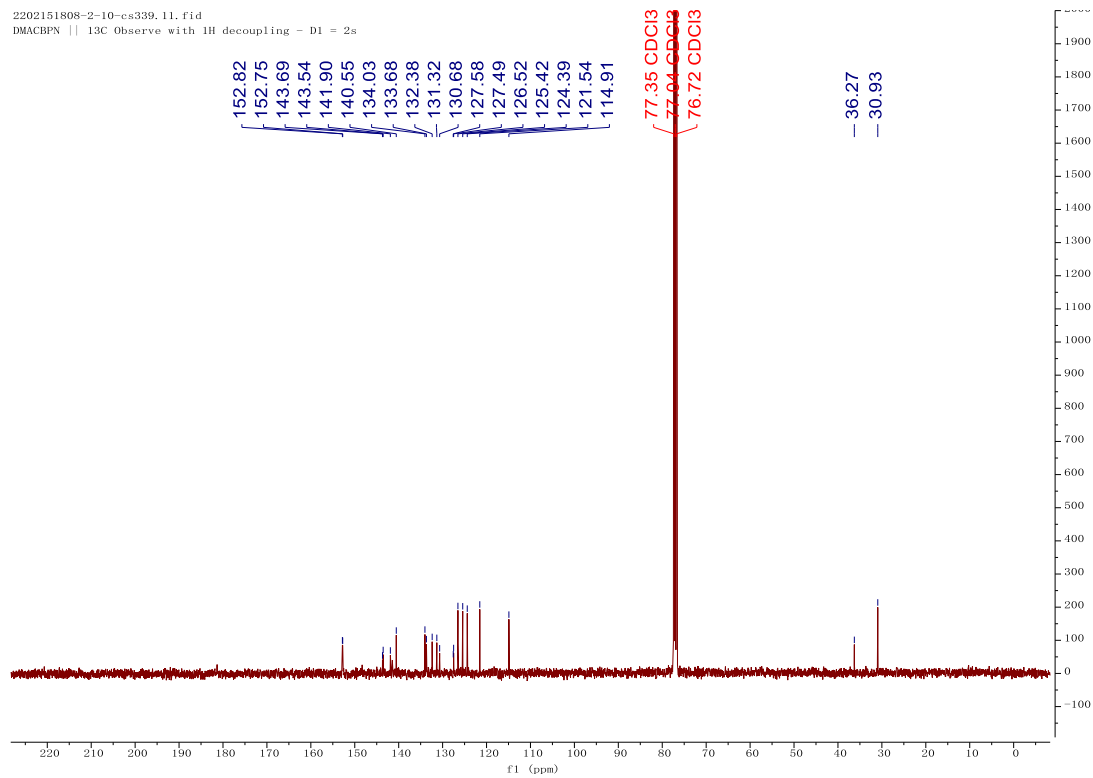


Figure S16. ^{13}C NMR spectra of DMACBPN in CDCl_3 .

Generic Display Report (all)

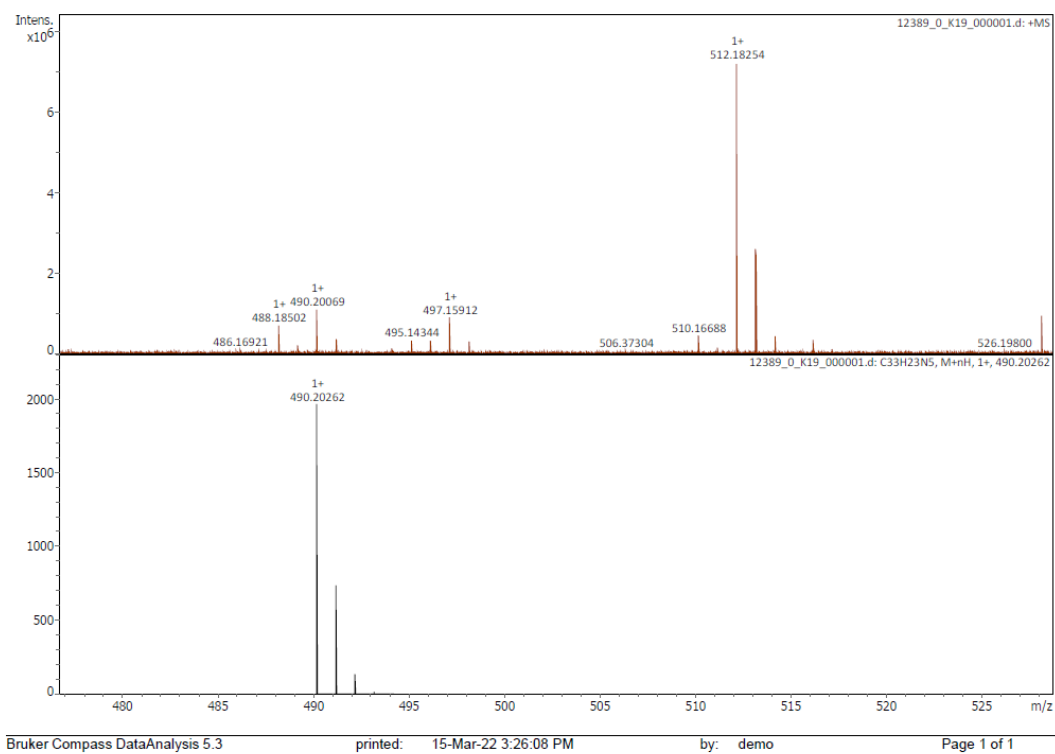


Figure S17. HRMS of DMACBPN.

Elemental Analysis Service Request Form

Researcher name Changfeng Si

Researcher email cs339@st-andrews.ac.uk

NOTE: Please submit ca. 10 mg of sample

Sample reference number	CFS-234-DMACBPN
Name of Compound	DMACBPN
Molecular formula	C33H23N5
Stability	
Hazards	
Other Remarks	

Analysis type:

Single Duplicate Triplicate

Analysis Result:

Element	Expected %	Found (1)	Found (2)	Found (3)
Carbon	80.96	79.87	81.09	
Hydrogen	4.74	4.73	4.77	
Nitrogen	14.31	13.63	13.81	
Oxygen				

Authorising Signature:

Date completed	30.03.22
Signature	S - P L
comments	-

Figure S18. EA trace of DMACBPN.

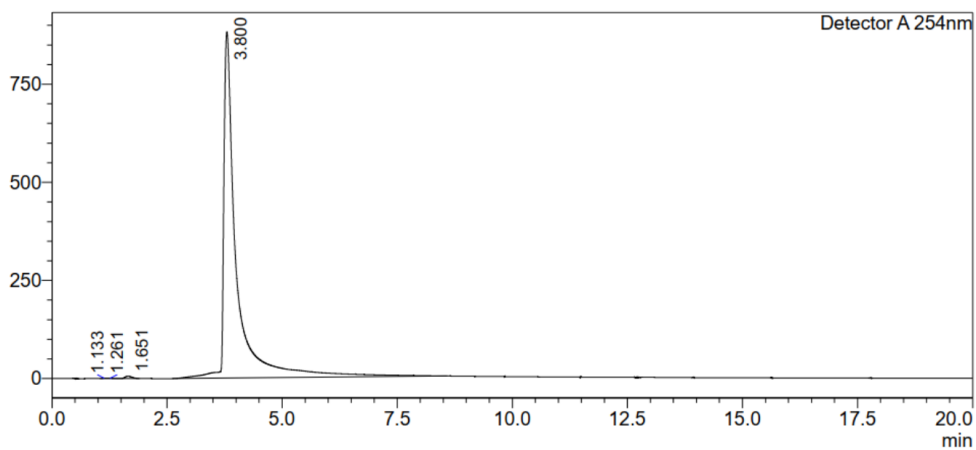
HPLC Trace Report 15 Jan 2023

<Sample Information>

Sample Name : DMACBPN
Sample ID :
Method Filename : 98% Methanol 2 Water 20 mins-NEW.lcm
Batch Filename : DMACBPN3-MeOH.lcb
Vial # : 1-9
Injection Volume : 60 uL
Date Acquired : 15/01/2023 17:52:14
Date Processed : 15/01/2023 18:12:16
Sample Type : Unknown
Acquired by : System Administrator
Processed by : System Administrator

<Chromatogram>

mV



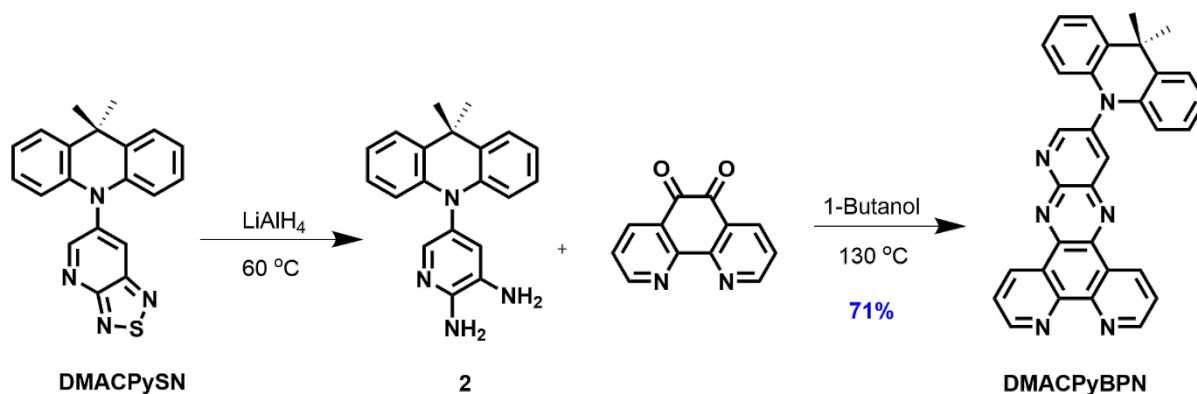
<Peak Table>

Detector A 254nm

Peak#	Ret. Time	Area	Height	Area%	Area/Height	Width at 5% Height
1	1.133	6662	1094	0.039	6.092	--
2	1.261	5379	773	0.032	6.960	--
3	1.651	60325	6076	0.355	9.928	0.312
4	3.800	16912219	880670	99.574	19.204	0.852
Total		16984584	888613	100.000		

Figure S19. HPLC trace of DMACBPN.

Synthesis of 12-(9,9-dimethylacridin-10(9*H*)-yl)pyrido[2',3':5,6]pyrazino[2,3-*f*][1,10]phenanthroline (DMACPyBPN):



Compound **DMACPyBPN** was synthesized according to the same procedure as described above for the synthesis of **DMACPyBP**, except that 1,10-phenanthroline-5,6-dione (0.306 g, 1.46 mmol) was used as the reactant instead of phenanthrene-9,10-dione, yielding a red solid (Yield = 0.510 g).

12-(9,9-dimethylacridin-10(9*H*)-yl)pyrido[2',3':5,6]pyrazino[2,3-*f*][1,10]phenanthroline (DMACPyBPN): $R_f = 0.2$ (33% DCM/Hexane). **Yield:** 71%. **Mp** = 325-326 °C. $^1\text{H NMR}$ (500 MHz, $\text{DMSO-}d_6$) δ 9.63 (dd, $J = 8.1, 1.8$ Hz, 1H), 9.54 (dd, $J = 8.1, 1.8$ Hz, 1H), 9.35 – 9.26 (m, 3H), 9.04 (d, $J = 2.7$ Hz, 1H), 8.02 (ddd, $J = 18.0, 8.1, 4.4$ Hz, 2H), 7.65 – 7.57 (m, 2H), 7.09 – 7.00 (m, 4H), 6.56 – 6.47 (m, 2H), 1.72 (s, 6H). $^{13}\text{C NMR}$ (126 MHz, DMSO) δ 158.67, 153.49, 153.38, 148.92, 148.73, 148.59, 143.56, 142.42, 140.34, 139.18, 139.05, 138.86, 134.15, 133.90, 131.68, 127.32, 127.26, 126.93, 126.26, 125.36, 125.27, 122.36, 115.36, 40.40, 40.23, 40.06, 39.90, 39.73, 39.56, 39.40, 36.35, 31.50. **HR-MS** $[\text{M}+\text{H}]^+$ **Calculated:** ($\text{C}_{32}\text{H}_{22}\text{N}_6$) 490.1906; **Found:** 490.1978. **Anal. Calcd. for $\text{C}_{32}\text{H}_{22}\text{N}_6$:** C, 78.35%; H, 4.52%; N, 17.13%. **Found:** C, 78.38%; H, 4.55%; N, 16.42%. **HPLC analysis:** 97.96% pure on HPLC analysis, retention time 4.84 minutes in 95% Acetonitrile 5% water.

Generic Display Report (all)

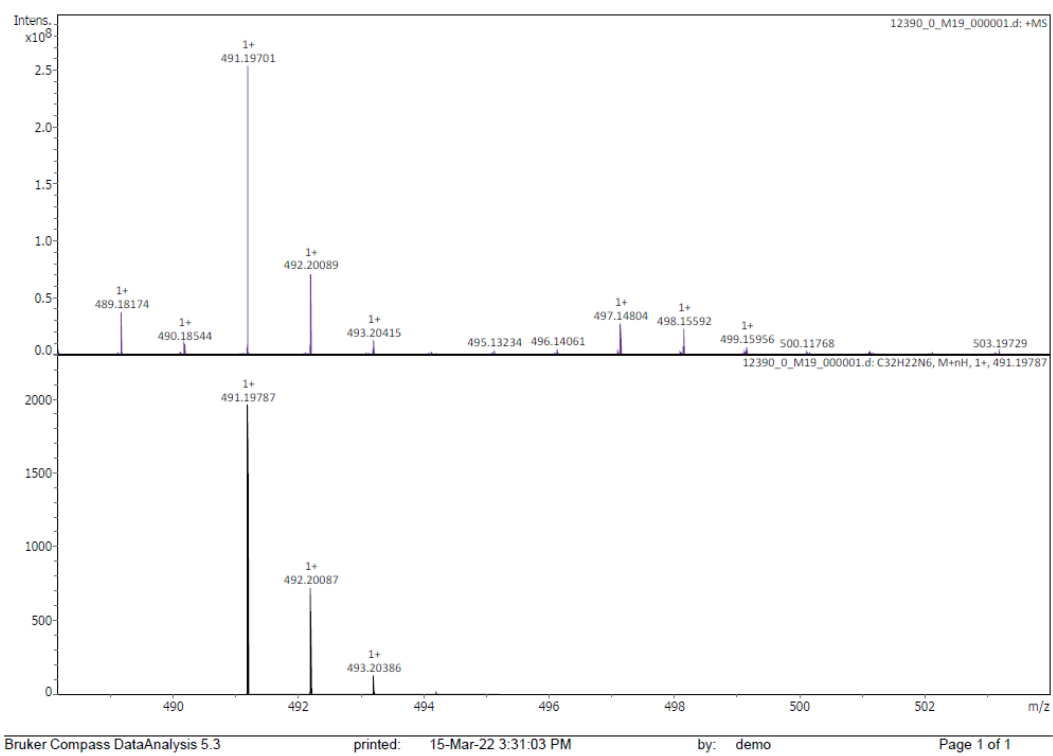


Figure S22. HRMS of DMACPyBPN.

Elemental Analysis Service Request Form

Researcher name Changfeng Si

Researcher email cs339@st-andrews.ac.uk

NOTE: Please submit ca. 10 mg of sample

Sample reference number	CFS-236-DMACPyBPN
Name of Compound	DMACPyBPN
Molecular formula	C32H22N6
Stability	
Hazards	
Other Remarks	

Analysis type:

Single Duplicate Triplicate

Analysis Result:

Element	Expected %	Found (1)	Found (2)	Found (3)
Carbon	78.35	78.58	78.17	
Hydrogen	4.52	4.62	4.55	
Nitrogen	17.13	16.42	16.36	
Oxygen				

Authorising Signature:

Date completed	30.03.22
Signature	S-PL
comments	-

Figure S23. HRMS of DMACPyBPN.

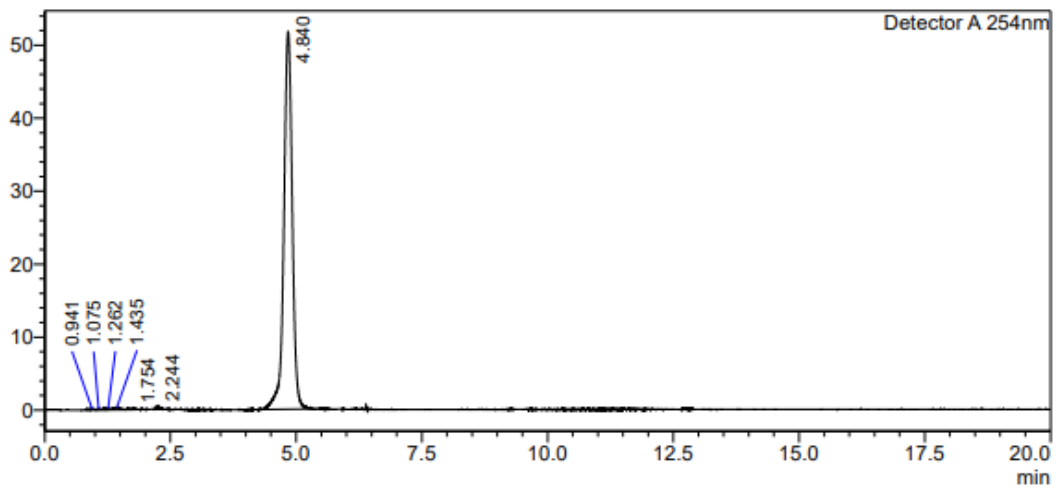
HPLC Trace Report25May2023

<Sample Information>

Sample Name : DMACPyBPN
Sample ID : DMACPyBPN
Method Filename : 95% Acetonitrile 5 Water 20 mins.lcm
Batch Filename : DMACPyBPN
Vial # : 1-53
Injection Volume : 10 uL
Sample Type : Unknown

<Chromatogram>

mV



<Peak Table>

Detector A 254nm

Peak#	Ret. Time	Area	Height	Area%	Area/Height	Width at 5% Height
1	0.941	1151	200	0.187	5.767	--
2	1.075	1107	162	0.180	6.838	--
3	1.262	2654	226	0.431	11.759	--
4	1.435	2672	317	0.434	8.417	--
5	1.754	2250	176	0.366	12.801	--
6	2.244	2713	431	0.441	6.295	--
7	4.840	602826	51622	97.961	11.678	0.421
Total		615371	53133	100.000		

Figure S24 . HPLC trace of DMACPyBPN.

3. DFT Calculations

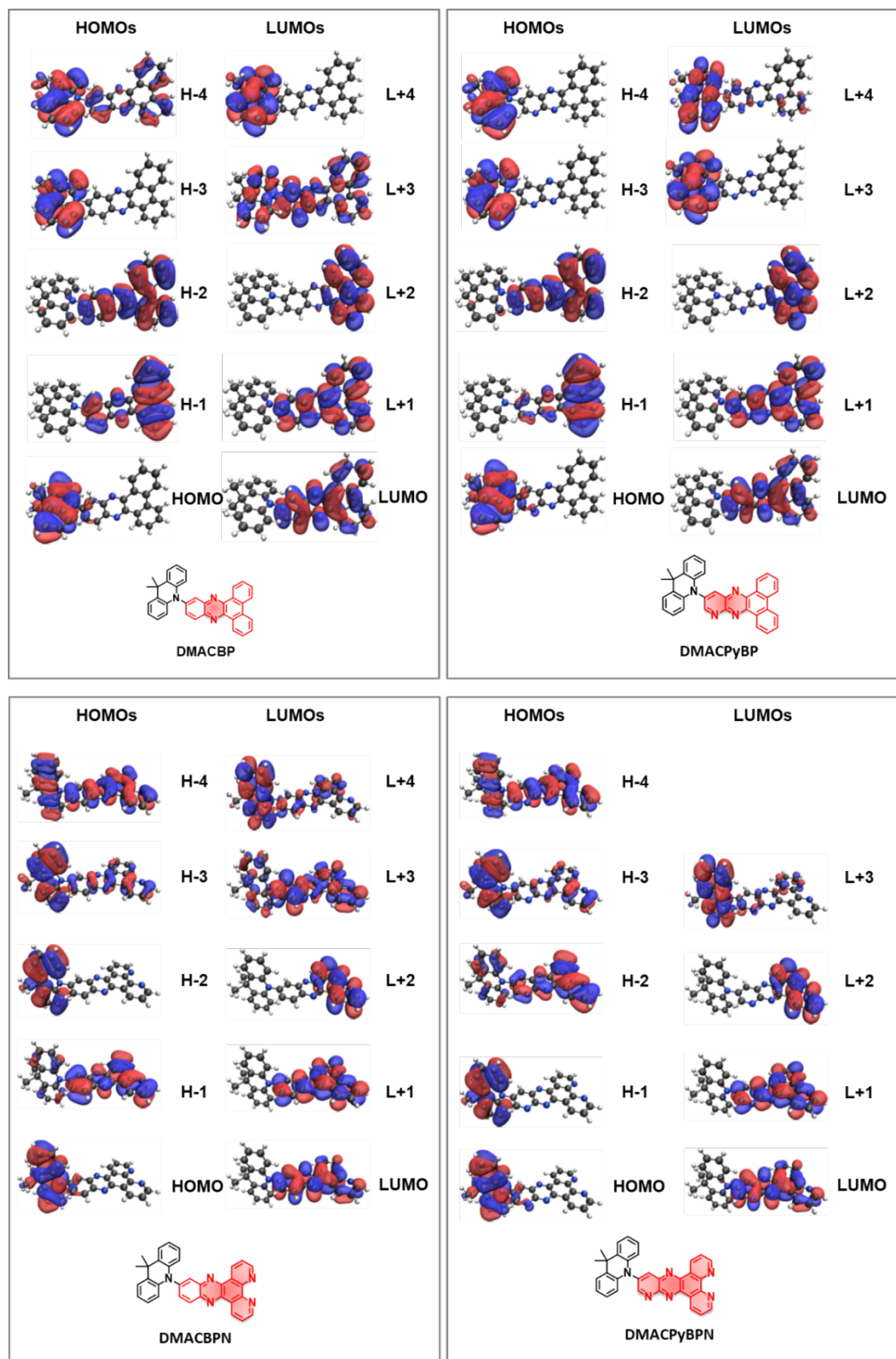


Figure S25. Calculated distribution of molecular orbitals for **DMACBP**, **DMACPyBP**, **DMACBPN** and **DMACPyBPN**. (isovalue= 0.02).

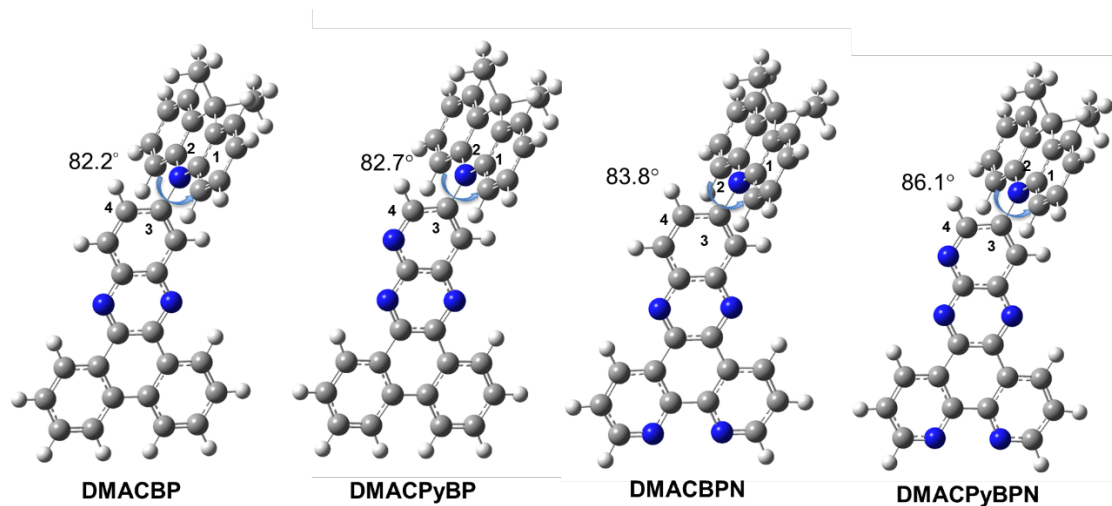


Figure S26. DFT-optimized molecular geometries of ground state of **DMACBP**, **DMACPyBP**, **DMACBPN** and **DMACPyBPN**.

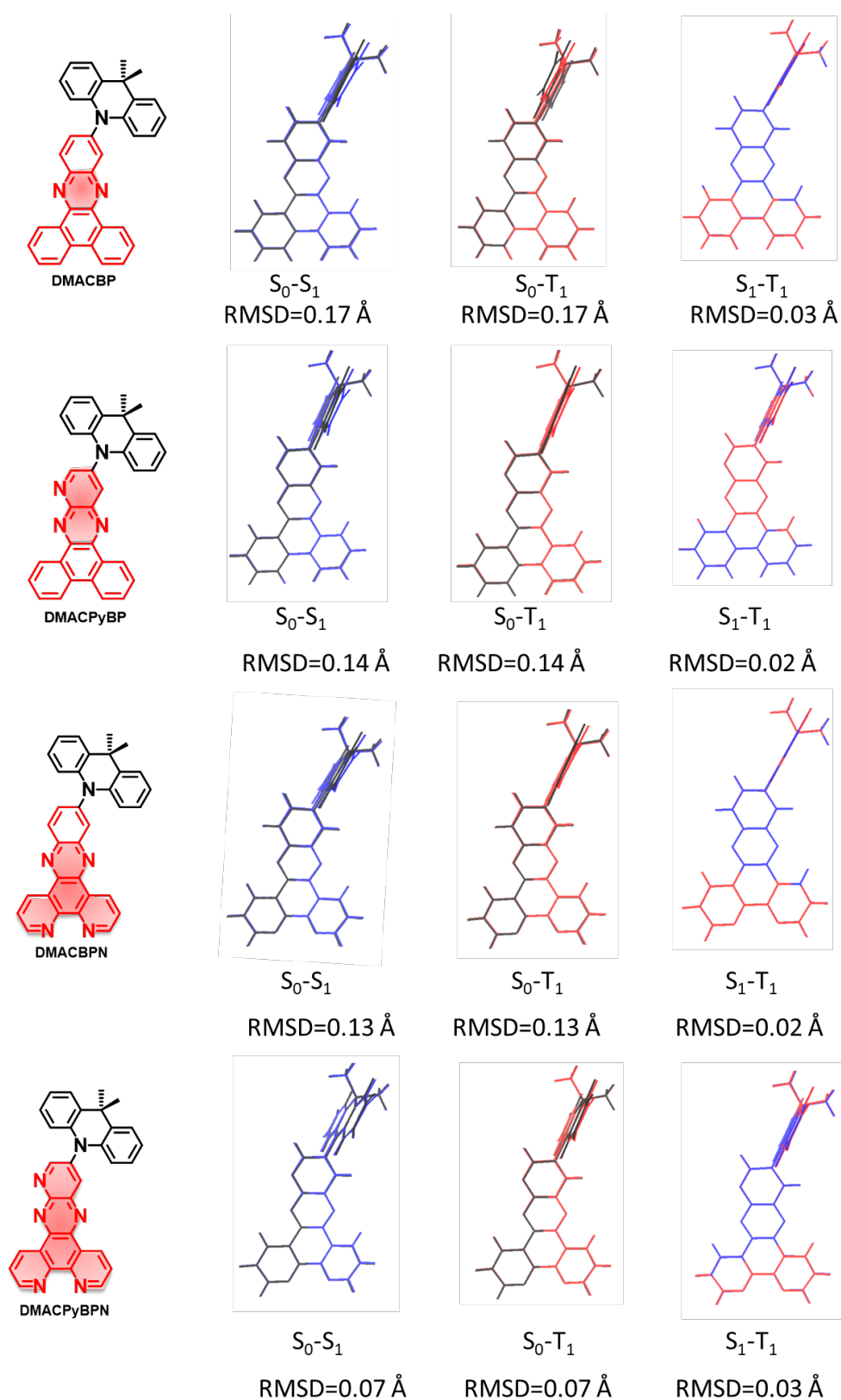


Figure S27. Calculated geometric changes between S_0 (black), S_1 (blue) and T_1 (red) states. (isovalue= 0.02).

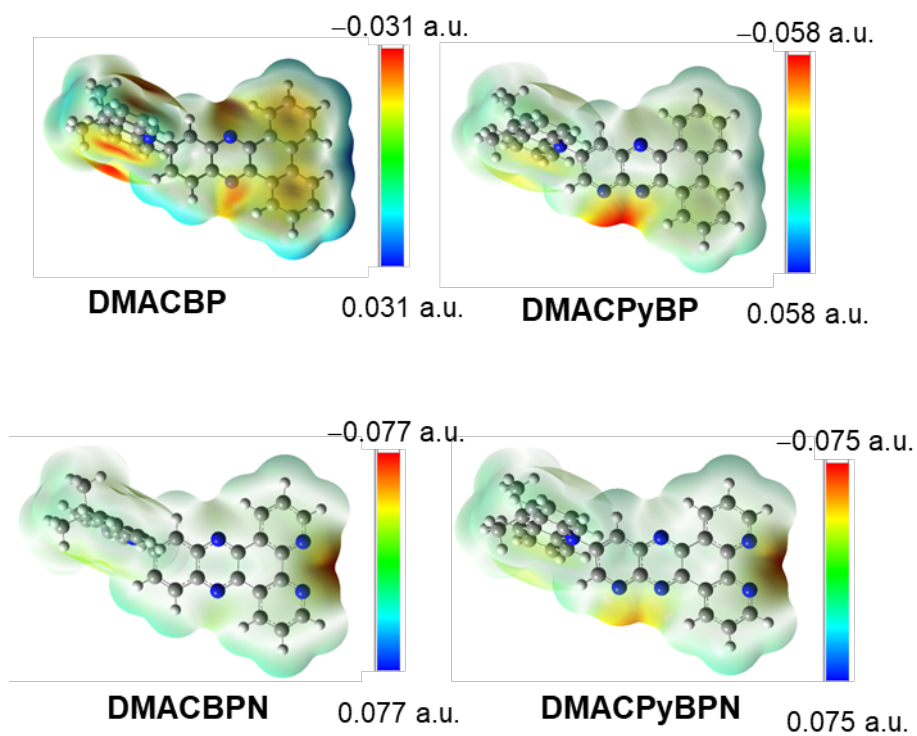


Figure S28. Electrostatic potential maps of **DMACBP**, **DMACPyBP**, **DMACBPN** and **DMACPyBPN** in ground states with an isodensity surface of 0.004.

4. Photophysical Properties

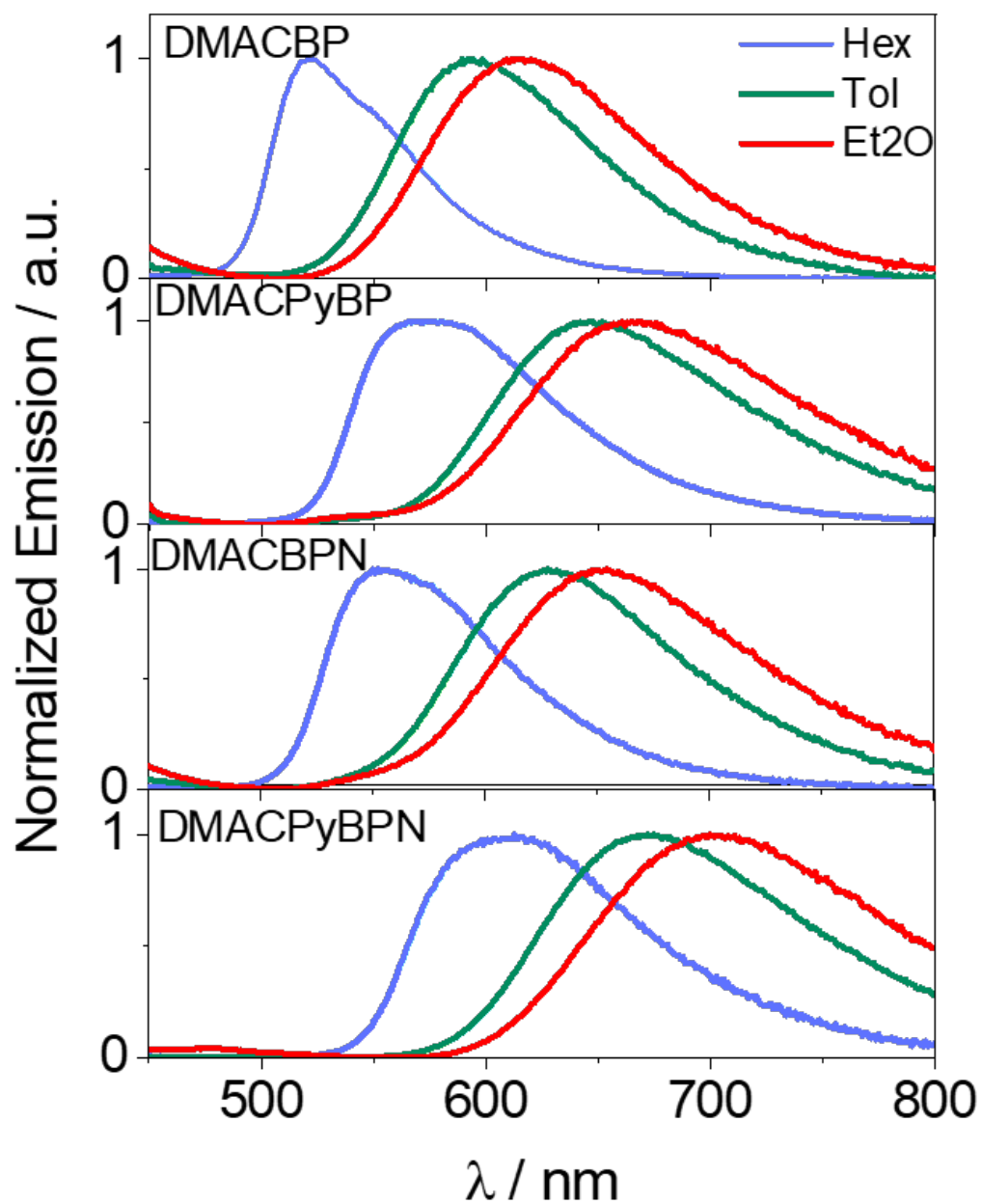


Figure S29. PL solvatochromism study of **DMACBP**, **DMACPyBP**, **DMACBPN** and **DMACPyBPN** ($\lambda_{\text{exc}} = 340 \text{ nm}$).

Table S1. Summary of solvatochromic PL study of **DMACBP**, **DMACPyBP**, **DMACBPN** and **DMACPyBPN**.

Compound	Solvent	$\lambda_{\text{PL}}^{\text{a}}$ / nm	FWHM^b / nm
DMACBP	Hexane	520	69
	Toluene	595	101
	Et ₂ O	615	115
DMACPyBP	Hexane	575	102
	Toluene	645	130
	Et ₂ O	679	144
DMACBPN	Hexane	552	91
	Toluene	630	118
	Et ₂ O	654	133
DMACPyBPN	Hexane	605	116
	Toluene	672	137
	Et ₂ O	700	156

^a Peak value of PL spectra obtained under aerated conditions at 298 K, concentration 10^{-5} M; $\lambda_{\text{exc}} = 340$ nm. ^b Full wavelength at half maximum of corresponding PL spectra.

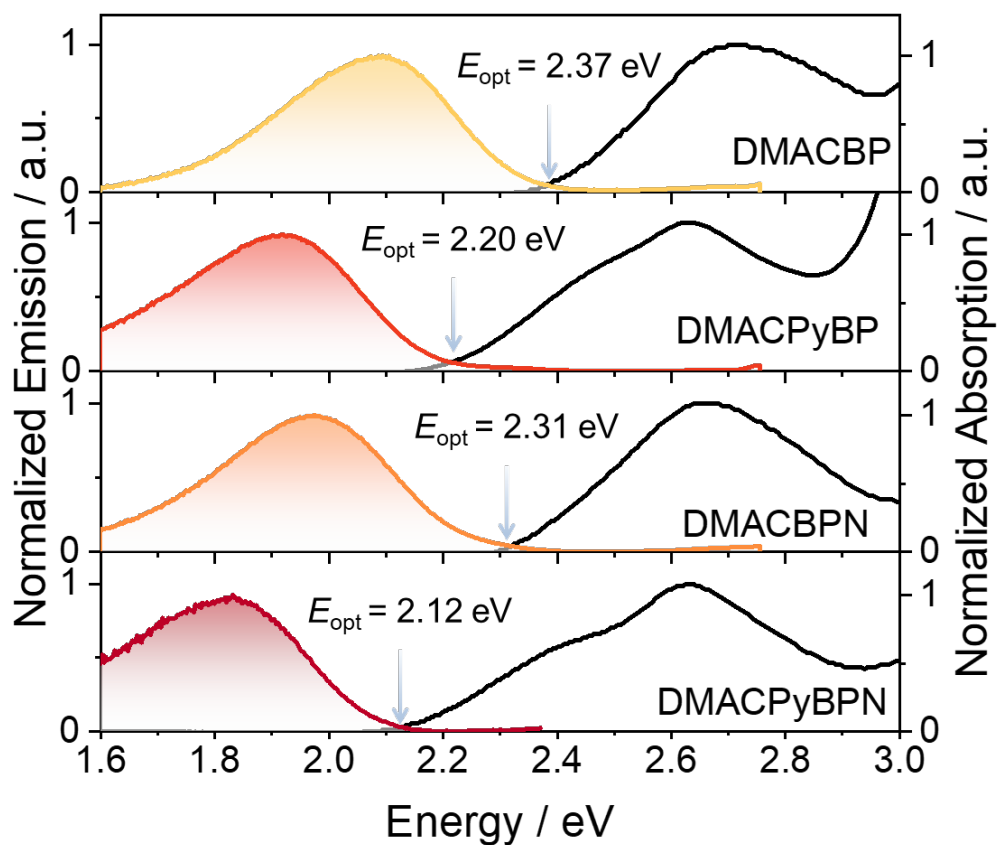


Figure S30. The optical bandgaps were determined from the intersection point of the normalized absorption and emission spectra for **DMACBP**, **DMACPyBP**, **DMACBPN** and **DMACPyBPN** ($\lambda_{\text{exc}} = 340$ nm).

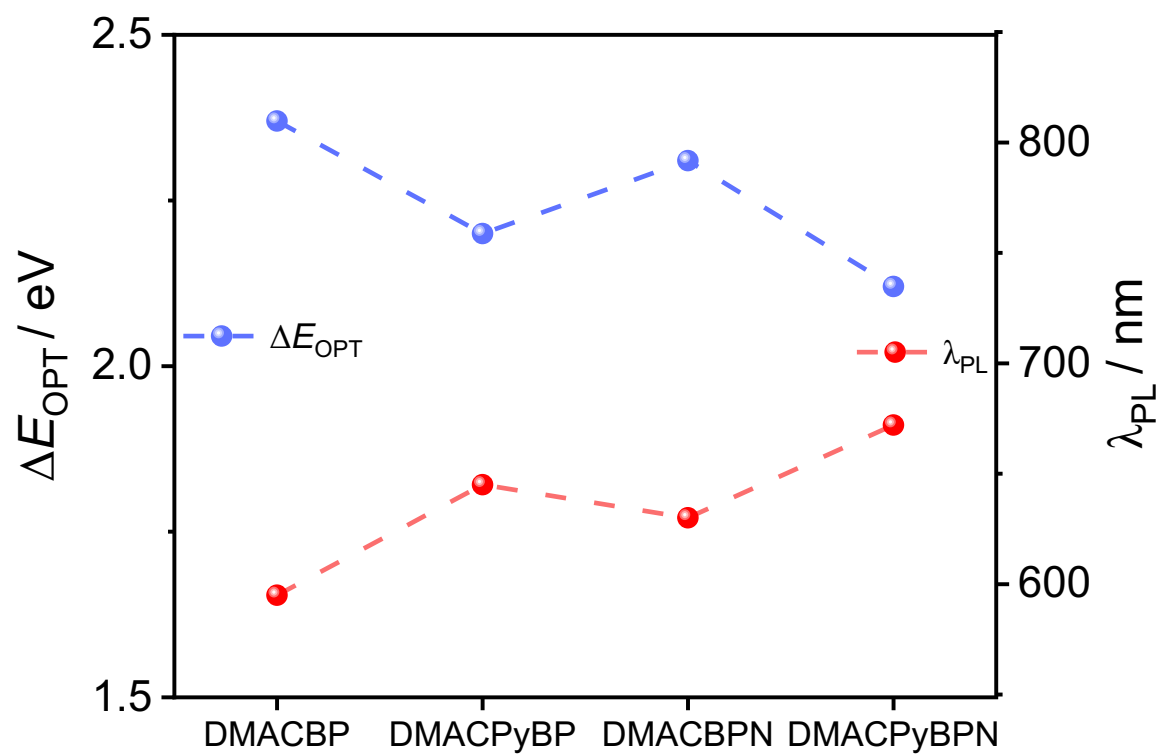


Figure S31. The relationship between the optical bandgaps and emission energies in toluene for **DMACBP**, **DMACPyBP**, **DMACBPN** and **DMACPyBPN** ($\lambda_{\text{exc}} = 340 \text{ nm}$).

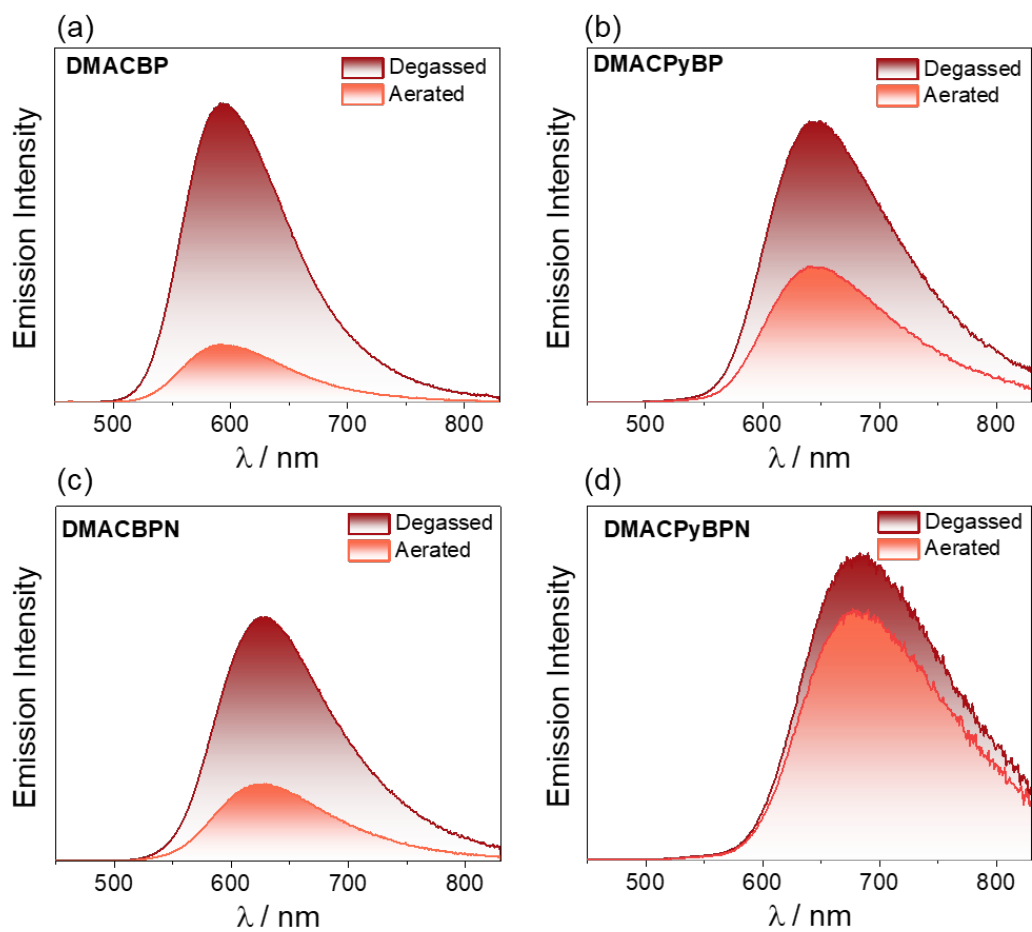


Figure S32. Steady-state PL spectra of (a) **DMACBP**, (b) **DMACPyBP**, (c) **DMACBPN** and (d) **DMACPyBPN** in degassed and aerated toluene ($\lambda_{\text{exc}} = 340 \text{ nm}$).

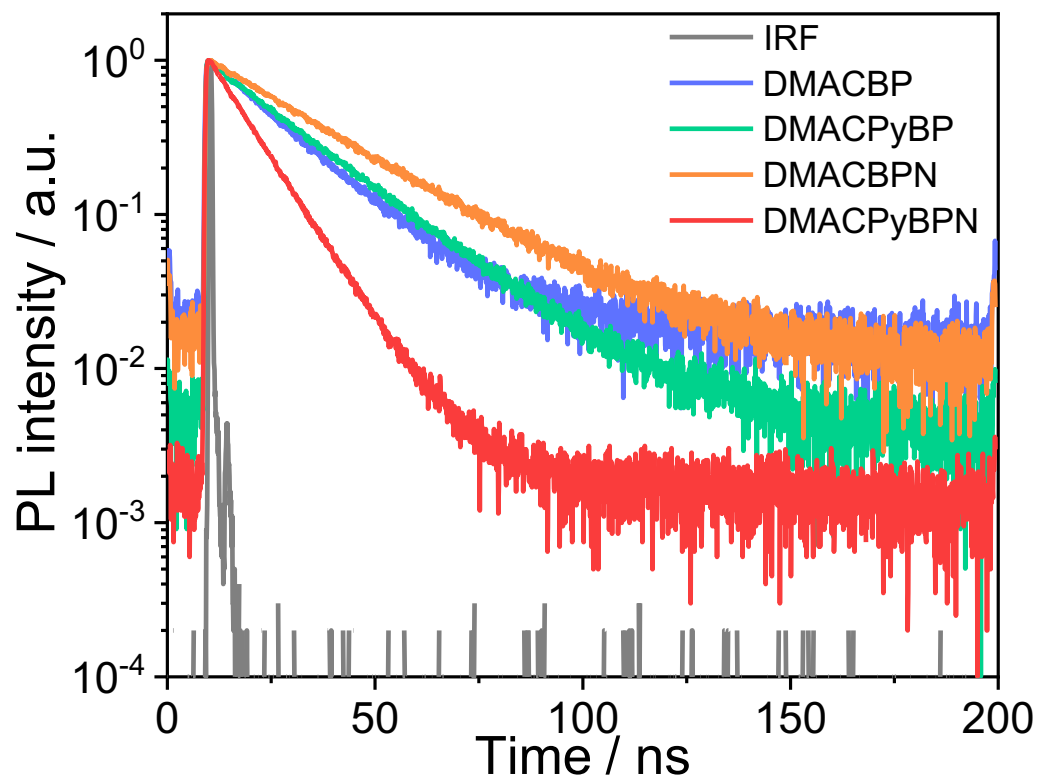


Figure S33. Time-resolved PL decay (time window 200 ns) of **DMACBP**, **DMACPyBP**, **DMACBPN** and **DMACPyBPN** in toluene ($\lambda_{\text{exc}}=375$ nm).

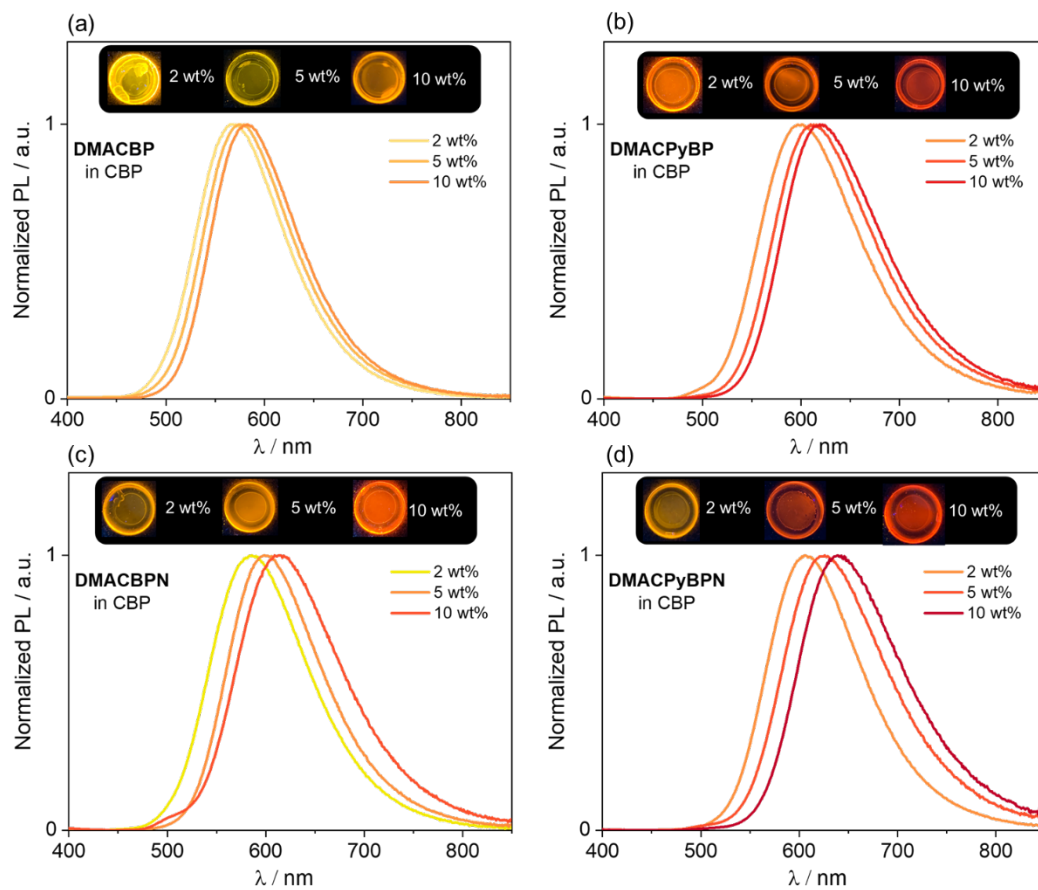


Figure S34. PL spectra of the **DMACBP**, **DMACPyBP**, **DMACBPN** and **DMACPyBPN** at different doping concentrations at room temperature ($\lambda_{\text{exc}} = 340 \text{ nm}$).

Table S2. Summary of Φ_{PL} of **DMACBP**, **DMACPyBP**, **DMACBPN** and **DMACPyBPN** at varying dopant concentration from 2–10 wt% in CBP.

Compound	Host	doped ratio ^a	$\Phi_{\text{PL}} / \%$ (in N ₂)	$\Phi_{\text{PL}} / \%$ (in Air)	λ_{PL}
DMACBP	CBP	2%	75	56	568
		5%	70	52	574
		10%	66	43	583
DMACPyBP	CBP	2%	47	41	601
		5%	43	40	610
		10%	41	36	620
DMACBPN	CBP	2%	71	52	586
		5%	67	48	598
		10%	64	46	615
DMACPyBPN	CBP	2%	37	30	606
		5%	36	31	625
		10%	29	25	639

^a Spin-coated 2–10 wt% emitters doped in CBP films and Φ_{PL} values were determined using an integrating sphere ($\lambda_{\text{exc}}=340$ nm).

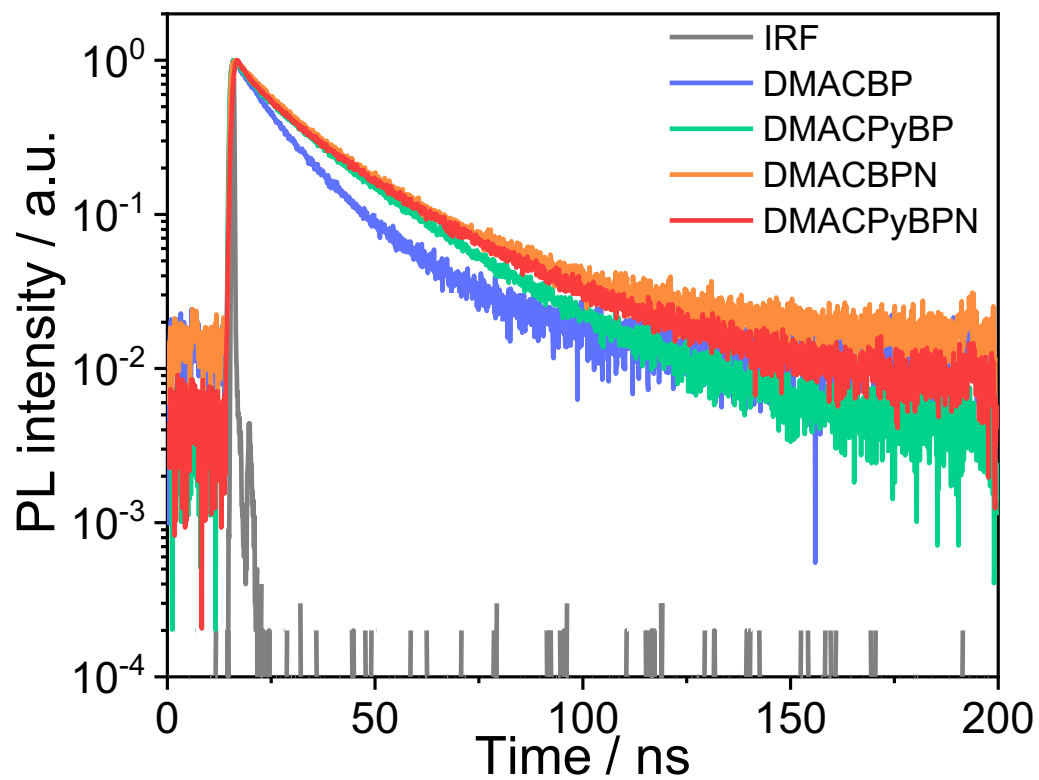


Figure S35. Time-resolved PL decay (time window 200 ns) of **DMACBP**, **DMACPyBP**, **DMACBPN** and **DMACPyBPN** in 2 wt% CBP film ($\lambda_{exc}=375$ nm).

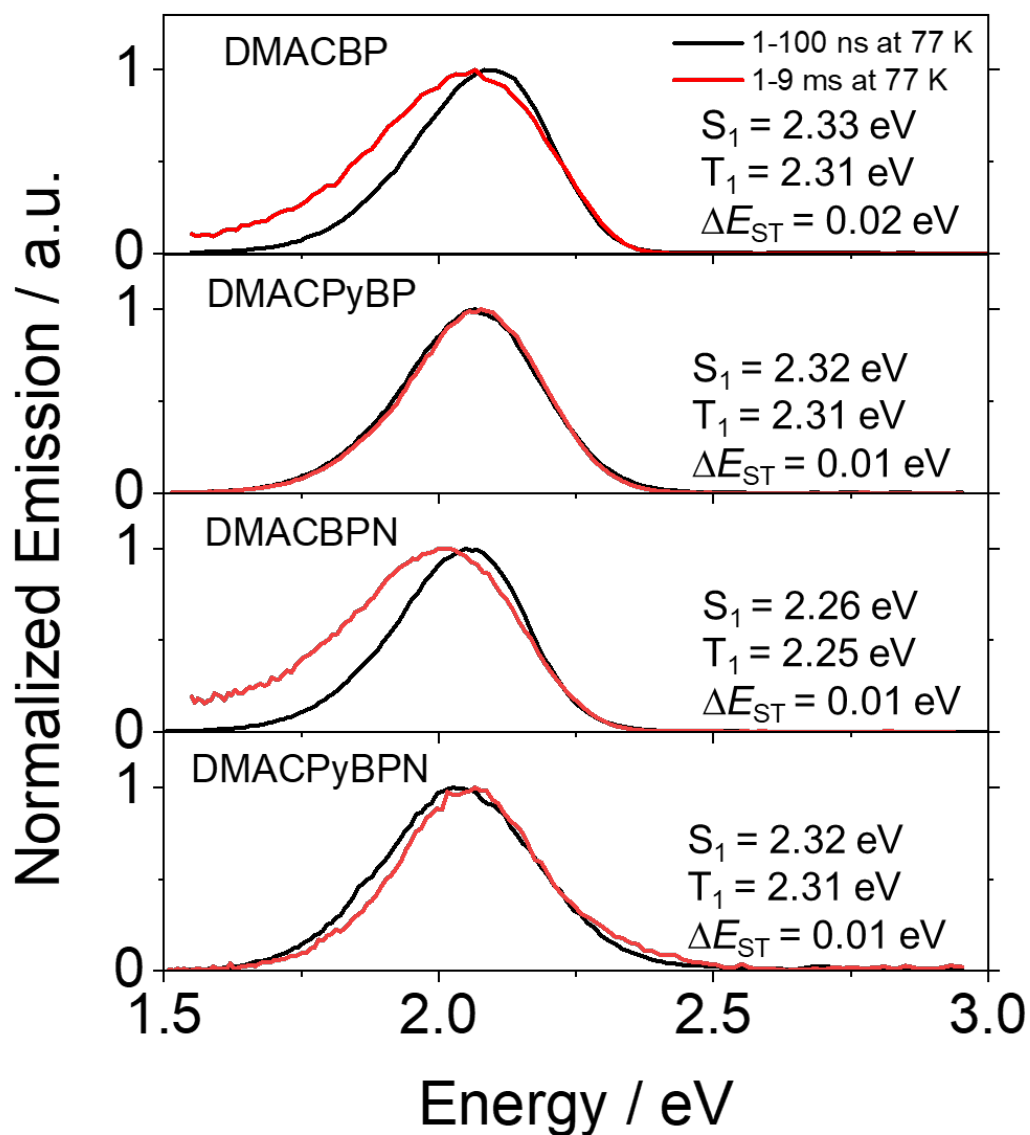


Figure S36. Prompt fluorescence (1-100 ns) and phosphorescence spectra (9-10 ms) of the **DMACBP**, **DMACPyBP**, **DMACBPN** and **DMACPyBPN** in 2 wt% doped films in CBP at 77 K ($\lambda_{exc} = 340$ nm).

5. OLED Fabrication and Characterization

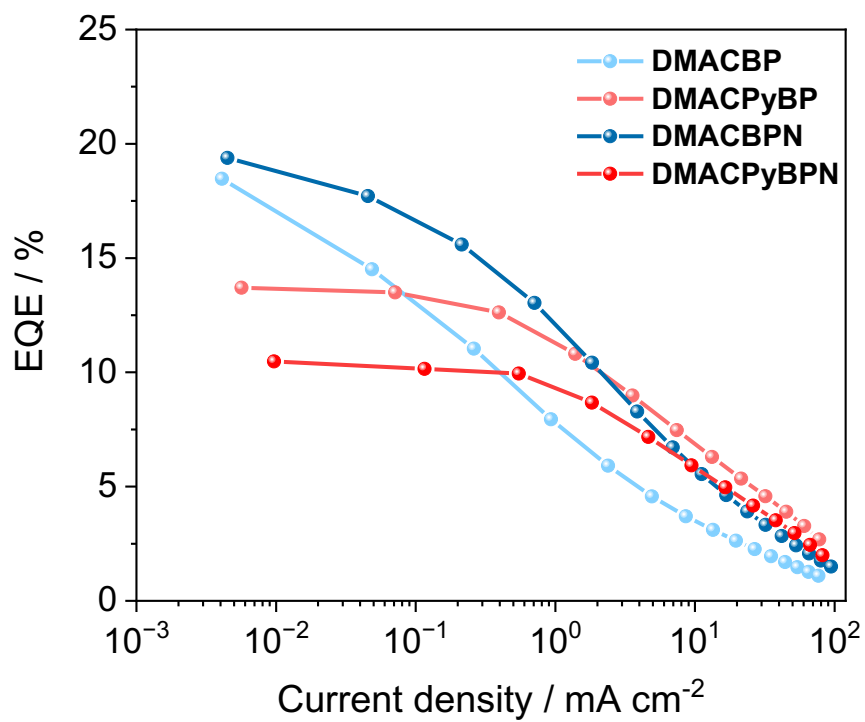


Figure S37. External quantum efficiency versus current density for the devices at 2 wt% emitter doping in CBP as the EML.

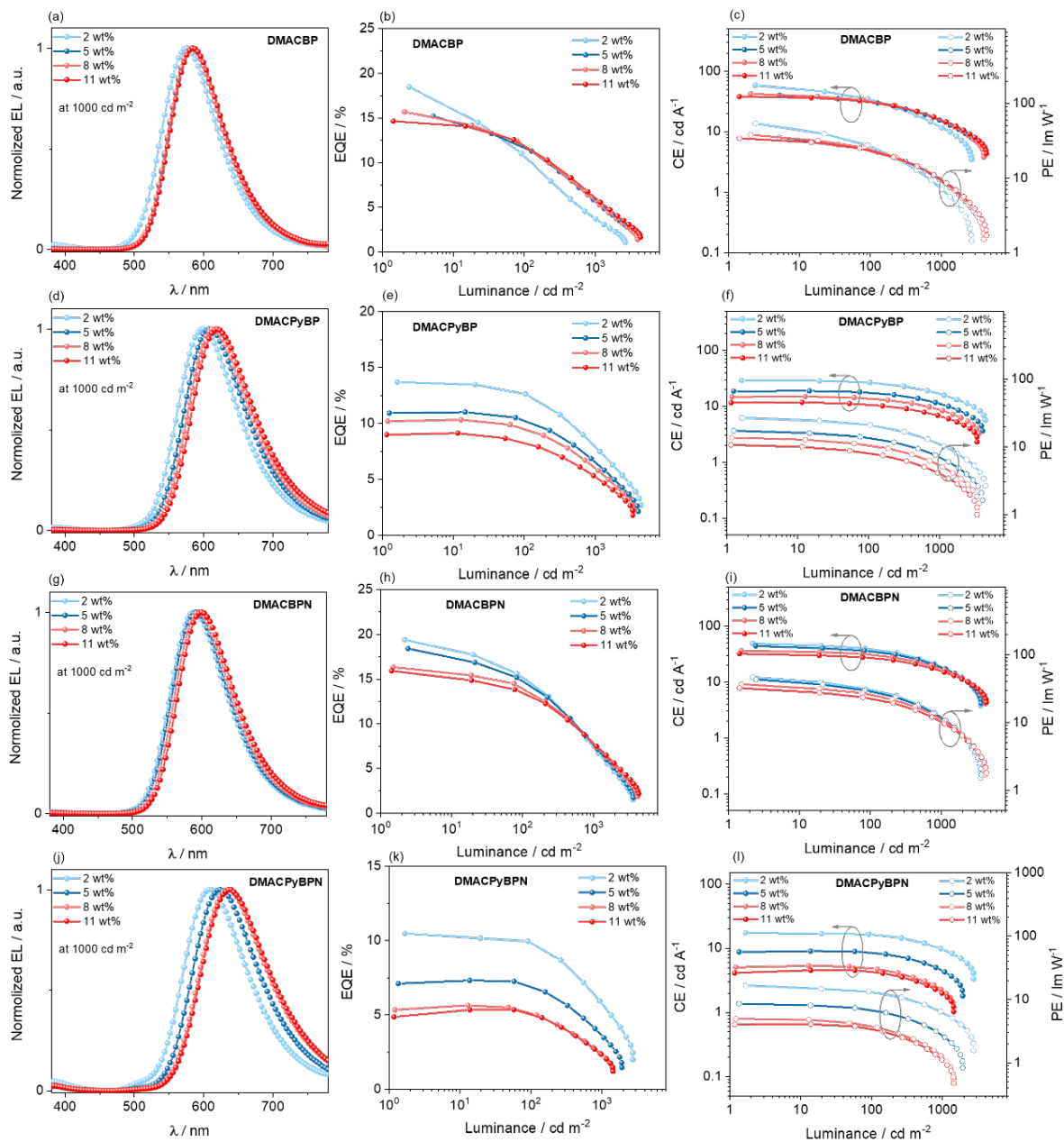


Figure S38. OLED performance using **DMACBP**, **DMACPyBP**, **DMACBPN** and **DMACPyBPN** at 2 wt%, 5 wt%, 8 wt% and 11 wt% doping in CBP as EML.

Table S3. Electroluminescence data for the devices

Emitter	Concentration / wt%	V _{on} ^a /V	CE _{max} ^b /cd A ⁻¹	PE _{max} ^c /lm W ⁻¹	EQE _{max/100/1000} ^d /%	L _{max} ^e /cd m ⁻²	λ _{EL} ^f /nm	CIE ^g (x, y)
DMACBP	2.0%	3.4	58.7	54.2	18.5/11.0/3.7	2665	576	0.48, 0.50
	5.0%	3.4	40.3	35.1	15.2/12.1/5.4	4146	580	0.52, 0.47
	8.0%	3.5	42.4	38.1	15.7/11.8/5.3	3978	584	0.52, 0.48
	11.0%	3.5	38.1	34.2	14.6/12.0/5.6	4332	584	0.52, 0.47
DMACPyBP	2.0%	3.4	28.9	26.7	13.7/12.6/7.5	4346	600	0.56, 0.44
	5.0%	3.4	18.6	17.2	10.9/10.2/5.8	4045	608	0.58, 0.41
	8.0%	3.4	14.7	13.6	10.2/9.5/5.8	3583	616	0.60, 0.40
	11.0%	3.4	11.6	10.7	9.0/8.3/4.7	3369	620	0.61, 0.39
DMACBPN	2.0%	3.3	48.9	46.5	19.4/14.6/6.7	3551	588	0.53, 0.46
	5.0%	3.2	43.9	43.1	18.4/14.5/7.1	3647	592	0.54, 0.45
	8.0%	3.1	36.1	36.6	16.3/13.9/7.4	4160	596	0.55, 0.44
	11.0%	3.1	31.9	32.3	15.9/13.4/7.5	4315	600	0.57, 0.43
DMACBPN	2%	3.3	17.4	16.6	10.5/10.0/5.0	2723	608	0.57, 0.42
	5%	3.2	8.8	8.6	7.3/7.1/3.5	1918	624	0.61, 0.39
	8%	3.2	5.1	5.0	5.3/5.0/2.1	1421	636	0.62, 0.37
	11%	3.2	4.1	4.0	5.4/5.1/2.0	1428	640	0.63, 0.37

^a Voltage at 1 cd m⁻². ^b Maximum current efficiency. ^c Maximum power efficiency. ^d Maximum external quantum efficiency/ at 100 cd m⁻²/ at 1000 cd m⁻². ^e Maximum luminance. ^f EL emission peak at 1000 cd m⁻². ^g Commission Internationale de L'Éclairage coordinates.

6. References

- (1) Ma, Y. P.; Wang, G.; Zhao, M.; Shi, Z. F.; Miao, Y.; Cao, X. P.; Zhang, H. L. A Red Thermally Activated Delayed Fluorescence Emitter Based on Benzo[c][1,2,5]Thiadiazole. *Dye. Pigment.* **2023**, *212*, 111084. <https://doi.org/10.1016/j.dyepig.2023.111084>.
- (2) MJ Frisch, GW Trucks, HB Schlegel, GE Scuseria, MA Robb, JR Cheeseman, G Scalmani, V Barone, GA Petersson, HJRA Nakatsuji, X Li, M Caricato, AV Marenich, J Bloino, BG Janesko, R Gomperts, B Mennucci, HP Hratchian, JV Ortiz, AF Izmaylov, JL Sonnenberg, D W, D. F. Gaussian 16 Rev. C.01; Wallingford, CT, 2016. *Gaussian 16 rev. C.01* **2016**, 2016.
- (3) Adamo, C.; Barone, V. Toward Reliable Density Functional Methods without Adjustable Parameters: The PBE0 Model. *J. Chem. Phys.* **1999**, *110* (13), 6158–6170. <https://doi.org/10.1063/1.478522>.
- (4) Petersson, G. A.; Tensfeldt, T. G.; Montgomery, J. A. A Complete Basis Set Model Chemistry. III. The Complete Basis Set-Quadratic Configuration Interaction Family of Methods. *J. Chem. Phys.* **1991**, *94* (9), 6091–6101. <https://doi.org/10.1063/1.460448>.
- (5) Hirata, S.; Head-Gordon, M. Time-Dependent Density Functional Theory within the Tamm-Dancoff Approximation. *Chem. Phys. Lett.* **1999**, *314* (3–4), 291–299. [https://doi.org/10.1016/S0009-2614\(99\)01149-5](https://doi.org/10.1016/S0009-2614(99)01149-5).
- (6) Grimme, S. Density Functional Calculations with Configuration Interaction for the Excited States of Molecules. *Chem. Phys. Lett.* **1996**, *259* (1–2), 128–137. [https://doi.org/10.1016/0009-2614\(96\)00722-1](https://doi.org/10.1016/0009-2614(96)00722-1).
- (7) Dennington, R., Keith, T. A., Millam, J. M. GaussView Version 6. *Semichem Inc. Shawnee Mission KS.* **2019**, 2019.
- (8) Humphrey, W.; Dalke, A.; Schulten, K. VMD: Visual Molecular Dynamics. *J. Mol. Graph.* **1996**, *14* (1), 33–38. [https://doi.org/10.1016/0263-7855\(96\)00018-5](https://doi.org/10.1016/0263-7855(96)00018-5).
- (9) O’Boyle, N. M.; Hutchison, G. R. Cinfony - Combining Open Source Cheminformatics Toolkits behind a Common Interface. *Chem. Cent. J.* **2008**, *2* (1), 1–10. <https://doi.org/10.1186/1752-153X-2-24>.
- (10) O’Boyle, N. M.; Banck, M.; James, C. A.; Morley, C.; Vandermeersch, T.; Hutchison, G. R. Open Babel: An Open Chemical Toolbox. *J. Cheminform.* **2011**, *3* (1), 33. <https://doi.org/10.1186/1758-2946-3-33>.
- (11) Allouche, A. Software News and Updates Gabedit — A Graphical User Interface for Computational Chemistry Softwares. *J. Comput. Chem.* **2012**, *32*, 174–182. <https://doi.org/10.1002/jcc>.
- (12) Hunter, J. D. Matplotlib: A 2D Graphics Environment. *Comput. Sci. Eng.* **2007**, *9* (3), 90–95. <https://doi.org/10.1109/MCSE.2007.55>.
- (13) Schirmer, J. Beyond the Random-Phase Approximation: A New Approximation Scheme for the Polarization Propagator. *Phys. Rev. A* **1982**, *26* (5), 2395–2416. <https://doi.org/10.1103/PhysRevA.26.2395>.

- (14) Gao, X.; Bai, S.; Fazzi, D.; Niehaus, T.; Barbatti, M.; Thiel, W. Evaluation of Spin-Orbit Couplings with Linear-Response Time-Dependent Density Functional Methods. *J. Chem. Theory Comput.* **2017**, *13* (2), 515–524. <https://doi.org/10.1021/acs.jctc.6b00915>.
- (15) Trofimov, A. B.; Schirmer, J. An Efficient Polarization Propagator Approach to Valence Electron Excitation Spectra. *J. Phys. B At. Mol. Opt. Phys.* **1995**, *28* (12), 2299–2324. <https://doi.org/10.1088/0953-4075/28/12/003>.
- (16) Johnson, E. R.; Keinan, S.; Mori-Sánchez, P.; Contreras-García, J.; Cohen, A. J.; Yang, W. Revealing Noncovalent Interactions. *J. Am. Chem. Soc.* **2010**, *132* (18), 6498–6506. <https://doi.org/10.1021/ja100936w>.
- (17) Lu, T.; Chen, F. Multiwfn: A Multifunctional Wavefunction Analyzer. *J. Comput. Chem.* **2012**, *33* (5), 580–592. <https://doi.org/10.1002/jcc.22885>.
- (18) Connelly, N. G.; Geiger, W. E. Chemical Redox Agents for Organometallic Chemistry. *Chem. Rev.* **1996**, *96* (2), 877–910. <https://doi.org/10.1021/cr940053x>.
- (19) Pommerehne, J.; Vestweber, H.; Guss, W.; Mahrt, R. F.; Bäessler, H.; Porsch, M.; Daub, J. Efficient Two Layer Leds on a Polymer Blend Basis. *Adv. Mater.* **1995**, *7* (6), 551–554. <https://doi.org/10.1002/adma.19950070608>.
- (20) Demas, J. N.; Crosby, G. A. The Measurement of Photoluminescence Quantum Yields.1 A Review2. *J. Phys. Chem.* **1971**, *75* (8), 991–1024.
- (21) Fery-Forgues, S.; Lavabre, D. Are Fluorescence Quantum Yields so Tricky to Measure? A Demonstration Using Familiar Stationery Products. *J. Chem. Educ.* **1999**, *76* (9), 1260–1264. <https://doi.org/10.1021/ed076p1260>.
- (22) Melhuish, W. H. Quantum Efficiencies of Fluorescence of Organic Substances. *J. Phys. Chem.* **1961**, *65* (65), 229–235.